REFERENCES

Ahn, S.J., Lee, K.H., Kim, B.K., and Jeong, H.M. (2000) Morphology and physical properties of SAN/NBR blends: the effect of AN content in NBR. Journal of Applied Polymer Science, 78, 1861–1868.

Ashley, S. (2003) Artificial muscles. Scientific American, October, 2003.

Bar-Cohen, Y. (2004). Electroactive Polymer (EAP) Actuators as Artificial Muscles: Reality, Potential, and challenges. Washington: The International Society for Optical Engineering.

Blythe, T. and Bloor, D. (2005) Electrical properties of polymers. New York: Cambridge University.

Carpi, F., Chiarelli, P., Mazzoldi, A., and Rossi, D.D. (2003) Electromechanical characterisation of dielectric elastomer planar actuators: comparative evaluation of different electrode materials and different counterloads. Sensors and Actuators A, 107, 85–95.

Chakrabortya, S., Bandyopadhyaya, S., Ametaa, R., Mukhopadhyaya, R., and Deurib, A.S. (2006) Application of FTIR in characterization of acrylonitrile-butadiene rubber (nitrile rubber). Polymer Testing, 26, 38-41.

Chandrasekhar, P. (1999) Fundamnetals and Applications of Conducting Polymers Handbook. USA: Kluwer Academic Publishers.

Cho, M.S., Nam, J.D., Lee, Y., Choi, H.R., and Koo, J.C. (2006) Dry type conducting polymer actuator based on polypyrrole–NBR/Ionic Liquid System. Molecular Crystals and Liquid Crystals, 444, 241-246.

Cho, M.S., Seo, H.J., Nam, J.D., Choi, H.R., Koo, J.C, Song, K.G., and Lee, Y. (2006) A solid state actuator based on the PEDOT/NBR system. Sensors and Actuators B, in press.

Chotpattananont, D., Sirivat, A., and Jamieson, A.M. (2004) Electrorheological properties of perchloric acid-doped polythiophene suspensions. Colloid & Polymer Science, 282, 357–365.

Deependra, K., Shahid, A., and Seungyong, Y. (2004) Semiconducting and Metallic Polymers. Condensed matter physics II, 1-19.

Eid, M.A.M., and El-Nashar, D.E. (2006) Filling Effect of Silica on Electrical and Mechanical Properties of EPDM/NBR Blends. Polymer-Plastics Technology and Engineering, 45, 675–684.

Ganapathy, H.S., Kim, J.S.,. Jin, S.-H, Gal, Y.-S., and Lim, K. T. (2006) Synthesis and properties of novel fluorinated ester substituted polythiophenes. Synthetic Metals, 156, 70–74.

Gazotti W.A., Jr, Faez, R., and De Paoli M-A. (1999) Thermal and mechanical behaviour of a conductive elastomeric blend based on a soluble polyaniline derivative. European Polymer Journal, 35, 35-40.

George, S., Varughese, K.T., and Thomas, S. (1999) Dielectric properties of isotactic polypropylene/nitrile rubber blends: effects of blend ratio, filler addition, and dynamic vulcanization. Journal of Applied Polymer Science, 73, 255–270.

George, S. Varughese, K.T., and Thomas, S. (2000) Thermal and crystallisation behaviour of isotactic polypropylene/nitrile rubber blends. Polymer, 41, 5485–5503.

Halloran, A.O and Malley, F.O. (2004) Materials and Technologies for Artificial Muscle: A review for the mechatronic muscle project, Department of Electronic Engineering. National University of Ireland Galway, Ireland.

Hao, T. (2002) Electrorheological suspensions. Advances in Colloid and Interface Science, 97, 1-35.

Hao, T., Kawai, A., and Ikazaki, F. (1998) Mechanism of the Electrorheological Effect: Evidence from the Conductive, Dielectric, and Surface Characteristics of Water-Free Electrorheological Fluids. Langmuir, 14, 1256-1262.

Hiamtup, P., and Sirivat, A. (2005) Soft and flexible actuator based on electromechanical response of polyaniline particles embedded in cross-linked poly(dimethyl siloxane) networks. American Society of Mechanical Engineers, Materials Division (Publication) MD, 100, 301-304.

Hofmann, W. (1989) Rubber Technology Handbook. New York: Oxford University Press.

Ibarra, L., Marcos-Fernández, A., and Alzorriz. (2002) Mechanistic approach to the curing of carboxylated nitrile rubber (XNBR) by zinc peroxide/zinc oxide. Polymer, 43, 1649-1655.

Ikada, E. and Watanabe, T. (1972) Relaxation of Acrylonitrile-Butadiene Copolymers. Journal of Polymer Science: Polymer Chemistry Edition, 10, 3457-3467.

Kim, B., Chen, L., Gong, J., and Osada, Y. (1999) Titration Behavior and Spectral Transitions of Water-Soluble Polythiophene Carboxylic Acids. Macromolecules, 32, 3964-3969.

Kim, S.J., Kim, H., Park, S.J., and Kim, S. (2004) Shape change characteristics of polymer hydrogel based on polyacrylic acid/poly(vinyl sulfonic acid) in electric fields. Sensors and Actuators A, 115, 146–150.

Khunanuruksaphong, R., and Sirivatm, A. (2007) Acrylic Elastomer Blends for Electroactive application. Materials Science and Engineering A, Inpress.

Kumar, D., and Sharma, R.C. (1998) Advances in conductive polymers. European Polymer Journal, 34, 1053-1060.

Kyokane, J., Tsujimoto, N., Ishida, M., and Fukuma, M. (2005) Space charge characteristics of fullerenol and carbon nanotube doped polyurethane elastomer(PUE) actuators. Proceedings of 2005 International Symposium on Electrical Insulating Materials, Japan.

Li, Y., Vamvounis, G., and Holdcroft, S. (2001) Facile functionalization of poly(3-alkylthiophene)s via electrophilic substitution. Macromolecules, 34,141-143.

Liu, B., and Shaw, T.M. (2001) Electrorheology of filled silicone elastomers. Journal of Rheology, 45, 641-657.

Lokander, M., and Stenberg, B. (2003) Performance of isotropic magneto-rheological rubber materials. Polymer Testing, 22, 245–251.

Ma, W. and Cross, L.E. (2004) An experimental investigation of electromechanical response in a dielectric acrylic elastomer. Applied Physics A, 78, 1201–1204.

Madden, J.W., Vandesteeg, N.A., Anquetil, P.A., Madden, P.G.A., Takshi, A., Pytel, R.Z., Lafontaine, S.R., Wieringa, P.A., and Hunter, I.W. (2004) Artificial muscle technology: Physical principles and naval prospects. IEEE Journal of Oceanic Engineering, 29(3), 706-728.

McCullough, R.D. (1998) The chemistry of conducting polythiophenes. Advance Materials, 10, 93-116.

Moschou, E., Peteu, S., Bachas, L.G., Madou, M.J., and Daunert, S. (2004) Artificial muscle material with fast electroactuation under neutral pH conditions. Chemistry of Materials, 16, 2499-2502.

Moschou, E.A., Madou. M.J., Bachas, L.G., and Daunert, S. (2005) Voltage-switchable artificial muscles actuating at near neutral pH. Sensors and Actuators B, In press.

Mu, S., and Park, S.M. (1995) Preparation and characterization of polythiophene in aqueous solutions. Synthetic Metals, 69, 311-312.

Naimlang, S., and Sirivat, A. (2005) Electromechanical responses of poly (p-phenylene vinylene)/ polydimethylsiloxane blends. American Society of Mechanical Engineers, Materials Division (Publication) MD, 100, 305-308.

Pei, Q. and Inganas, O. (1992) Electrochemical application of the bending beam method. 1. Mass transport and volume changes in polypyrrole during redox. The Journal of Physical Chemistry, 96, 10507–10514.

Pelrine, R., Kornbluh, R., and Joseph, J. (1998) Electrostriction of polymer dielectrics with compliant electrodes as a means of actuation. Sensors and Actuators A: Physical, 64, 77–85.

Pelrine, R., Kornbluh, R., and Joseph, J. (2000) High-speed electrically actuated elastomers with strain greater than 100%. Science, 287, 836-839.

Plocharski, J., and Wyciślik, H. (2000) Mixed conductivity in poly(p-phenylene) doped with iron chloride. Solid State Ionics, 127, 337–3443.

Puvanatvattana, T., Chotpattananont, D., Hiamtup, P., Niamlang, S., Sirivat, A., and Jamieson, A. M. (2005) Electric field induced stress moduli in polythiophene/polyisoprene elastomer blends. Reactive & Functional Polymers, 66, 1575–1588.

Sau, K.P., Chaki, T.K., and Khastgir, D. (1999) Electrical and mechanical properties of conducting carbon black filled composites based on rubber and rubber blends. Journal of Applied Polymer Science, 71, 887–895.

Senadeera, G. K. R. (2005) Microwave-assisted steps in the synthesis of poly(3-thiophenylacetic acid). Current Science, 88, 145-148.

Shiga, T., Okada, A., and Kurauchi, T. (1993) Electroviscoelastic effect of polymer blends consisting of silicone elastomer and semiconducting polymer particles. Macromolecules, 26, 6958-6963.

Shiga, T. (1997) Deformation and Viscoelastic Behavior of Polymer Gels in Electric Fields. Advances in Polymer Science, 134, 133-163.

Soares, B.G., Amorim, G.S., Souza Jr.,F.G., Oliveira, M.G., and Pereira da Silva, J.E. (2006) The in situ polymerization of aniline in nitrile rubber. Synthetic Metals, 156, 91–98.

Thomsen D.L., Keller, P., Naciri, J., Pink, R., Jeon, H., Shenoy, D. and Ratna, B.R. (2001) Liquid crystal elastomers with mechanical properties of a muscle. Macromolecules, 34, 5868-5875.

Varghese, H., Johnson, T., Bhagawan, S.S., Joseph, S. Thomas, S., and Groeninckx, G. (2002) Dynamic mechanical behavior of acrylonitrile butadiene rubber/poly(ethylene-co-vinyl acetate) blends. Journal of Polymer Science: Part B: Polymer Physics, 40, 1556–1570.

Vallim, M.R., Felisberti, M.I., and De Paoli, M.-A. (1999) Blends of polyaniline with nitric rubber. Journal of Applied Polymer Science, 75, 677.

Yong, K.C., Foot, P.J.S., Morgan, H., Cook, S., and Tinker, A.J. (2006) Conductive poly(butadiene-co-acrylonitrile)-polyaniline dodecyl-benzenesulfonate [NBR- Ani.DBSA] blends prepared in solution. (2006) European Polymer Journal, 42, 1716–1727.

APPENDICES

Appendix A Identification of Characteristic FT-IR Spectrum of 3-Thiophene Acetic Acid, Poly(3-thiophene methyl acetate), Undoped Poly(3-thiophene acetic acid), Acrylonitirle-butadiene Rubber, and P3TAA/NBR Blends

The poly(3-thiophene acetic acid) (P3TAA) was first characterized by FT-IR spectroscopy in order to identify functional groups. Fourier Transform Infrared Spectrometer (Thermo Nicolet, Nexus 670) operated in the absorption mode with 32 scans and a resolution of 4 cm^{-1}, covering a wavenumber range of 4000-400 cm^{-1} using a deuterated triglycine sulfate detector. Optical grade KBr (Carlo Erba Reagent) was used as the background material. The synthesized PTAA was intimately mixed with dried KBr at a ratio of P3TAA: KBr = 1:20.
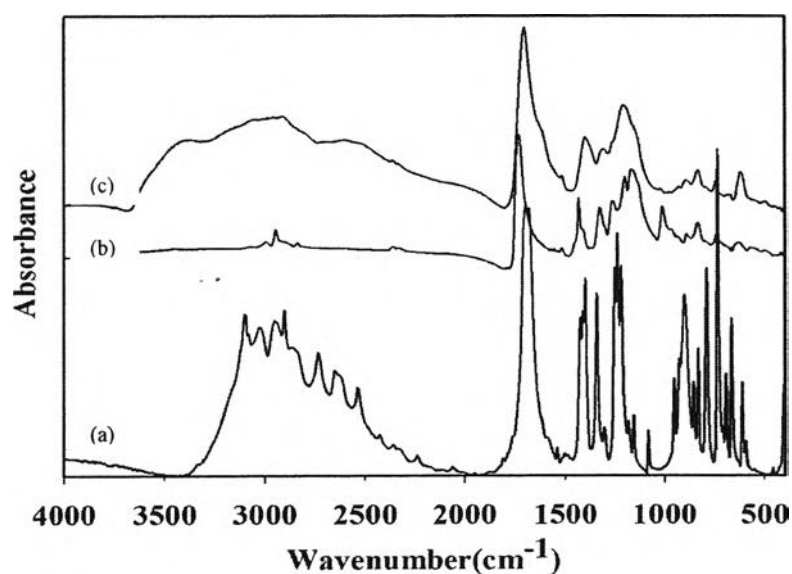
Figure A1 The FT-IR spectrum of: a) monomer; 3-thiophene acetic acid (TAA); b) Poly(3-thiophene methyl acetate(P3TMA); and (c) Poly(3-thiophene acetic cid) (P3TAA).

The assignments of peaks in the spectrum are shown in Table A1. The characteristic peaks of PTAA were found at 3200-3000 cm^{-1} assignable to the stretching vibration of the C-H bond on the thiophene ring; at 3000-2800 cm^{-1}, they

represent the aliphatic C-H bonds; at 1700 cm^{-1}, the C=O stretching vibration; at 1400 cm^{-1}, the thiophene ring stretching vibration; and at 1300-1200 cm^{-1}, the C-O strectching vibration. The most characteristic feature in this spectrum is the extremely broad O-H absorption occurring in the region from 3400 to 2400 cm^{-1}, which is attributed to the strong hydrogen bonding of the dimmer. This absorption often obscures the C-H stretching vibrations that occur in the same region. It is obvious from the absorption paek at around 1700 cm^{-1} that the ester groups were not deteriorated during the oxidative polymerization (Kim et al., 1999). The FT-IR spectrum of Poly(3-thiophenemethyl acetate);PTMA, shown at 3000-2800 cm^{-1} assigned to the stretching vibration of the C–H band on the thiophene ring. Absorption band at 1735-1750 cm^{-1} for the C=O stretching vibrations; at 1432 cm^{-1} for thiophene ring stretching vibration and at 1300–1200 cm^{-1} for C–O stretching vibrations. Therefore, the oxidative polymerization of 3-thiophane methyl acetate is confirmed (Senadeera, 2005).

Table A1 The FT-IR absorption spectrum of undoped and doped P3TAA

Wavenumber (cm^{-1})	Assignments	References
3400-2400 ± 20 [3400-2400]	O-H stretching vibration	Kim et al. (1999)
3100 ± 50 [3200 – 3000]	C-H stretching of thiophene ring	Kim et al. (1999)
2910 ± 10 [3000 – 2800]	C-H stretching of aliphatic	Kim et al. (1999)
1710 ± 10 [1700]	C=O stretching vibration	Kim et al. (1999)
1399 ± 5 [1400]	Thiophene ring stretching vibration	Kim et al. (1999)
1300 ± 5 1300 - 1200	C-O stretching vibration	Kim et al. (1999)

For Arcylonitrile butadiene rubber, were characterized in order to identify their structures in different types. FT-IR spectrometer Fourier transform (Thermo Nicolet, Nexus 670) operated in the absorption mode with 32 scans and a resolution of ± 4 cm^{-1}, covering a wavenumber range of 4000-400 cm^{-1} using a deuterated triglycine sulfate detector. A Horisontal Attenuated Total Reflectance accessory (HATR) with equipped with ZnSe was used. The characteristic peaks of Arcylonitrile butadiene rubber were found at 2850-3300 cm^{-1} assignable to the stretching vibration of the C-H bond. The characteristic absorptions at 2237 cm^{-1}(-C$\equiv$N stretching), 1630 cm^{-1}(C=C stretching) and 1440 -1445 cm^{-1} is out of plane C-H wagging (Yong, et al., 2006).
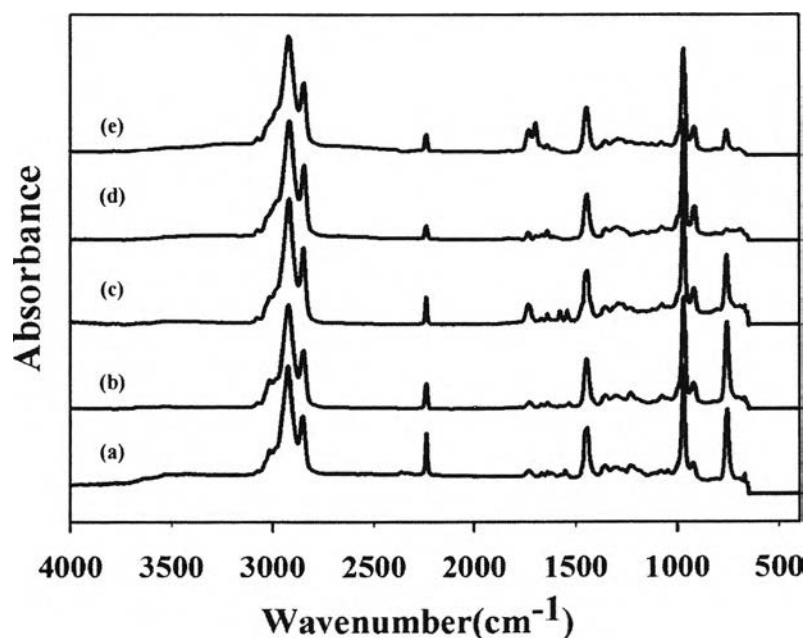
Figure A2 The FT-IR spectrum of: a) NBR1; b) NBR2; c) NBR3; d) NBR4 and e) NBR5.

Table A2 Summarized of FT-IR absorption spectrum at 2237 cm^{-1} (-C≡N)

Grade	Type	Bound acrylonitrile (%)	FTIR band intensity ratio
DN101L	NBR1	42.30	47%
Krynac3345 F	NBR2	33.00	23%
DN2850	NBR3	28.00	20%
DN401L	NBR4	18.50	13%
KrynacX7.50	NBR5	26.50	20%
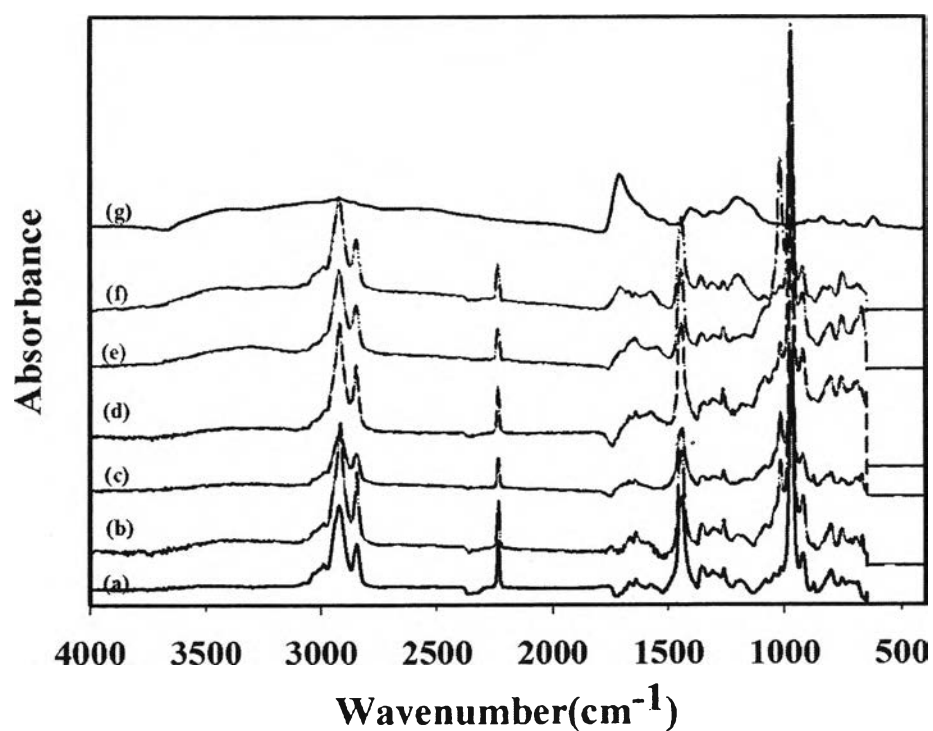
Figure A3 The FT-IR spectrum of: a) pure NBR1; b) P3TAA_5/NBR1; c) P3TAA_10/NBR1; d) P3TAA_15/NBR1; e) P3TAA_20/NBR1; f) P3TAA_30/NBR1 g) pure P3TAA.

Poly(3-thiopheneacetic acid)/Acrylonitrile butadiene rubber, P3TAA/NBR, blends were characterized by using FT-IR spectrometer Fourier transform (Thermo

Nicolet, Nexus 670) operated in the absorption mode with 32 scans and a resolution of ± 4 cm^{-1}, covering a wavenumber range of 4000-400 cm^{-1} using a deuterated triglycine sulfate detector. A Horisontal Attenuated Total Reflectance accessory (HATR) with equipped with ZnSe was used. The results showed the position wavenumber of the blends that were combined between NBR and P3TAA. When P3TAA were added to NBR matrix the wavenumber around 3400 cm^{-1} which represent –OH group of poly(3-thiopheneacetic acid) were detected at the blend films. The absorbance of this wavenumber was higher in the blends having high P3TAA composition.

Appendix B   Identification of Characteristic of Proton Nuclear Magnetic Resonance (^{1}H-NMR)

Proton Nuclear Magnetic Resonance (^{1}H-NMR) Varian Unity Inova was used to identify our successful synthesis of poly (3-thiopheneacetic acid). The different characteristic peaks of both polythiophene derivatives are shown in the figures B1 and B2.
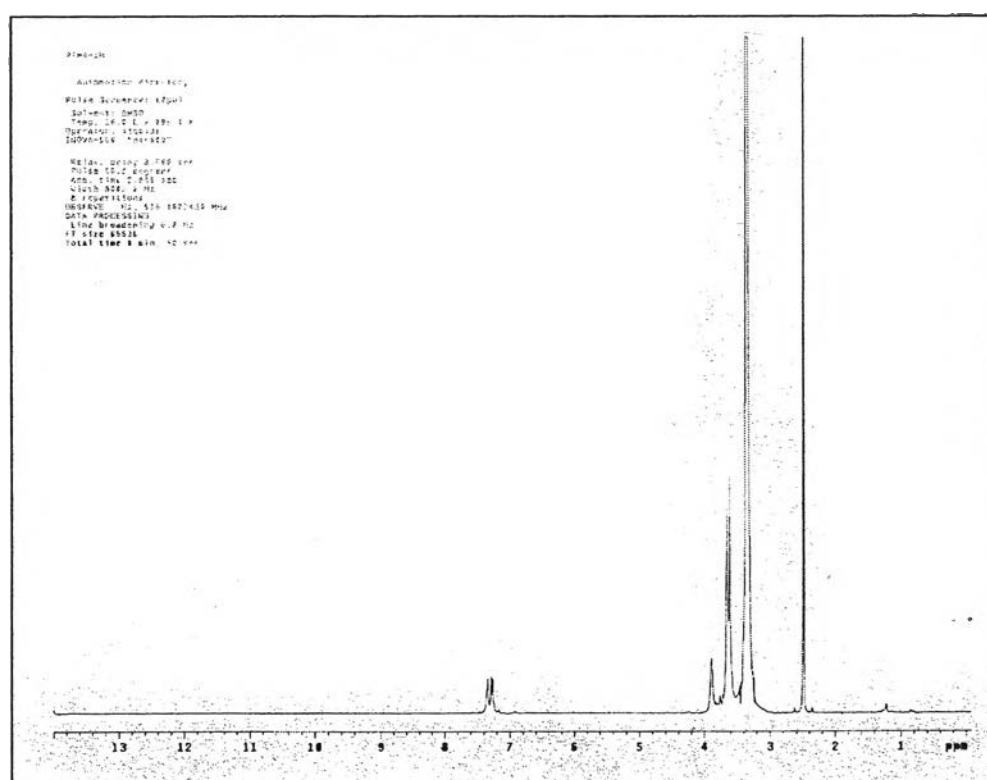
Figure B1 ^{1}H-NMR characteristic peaks of poly(3-thiophenemethyl acetate).
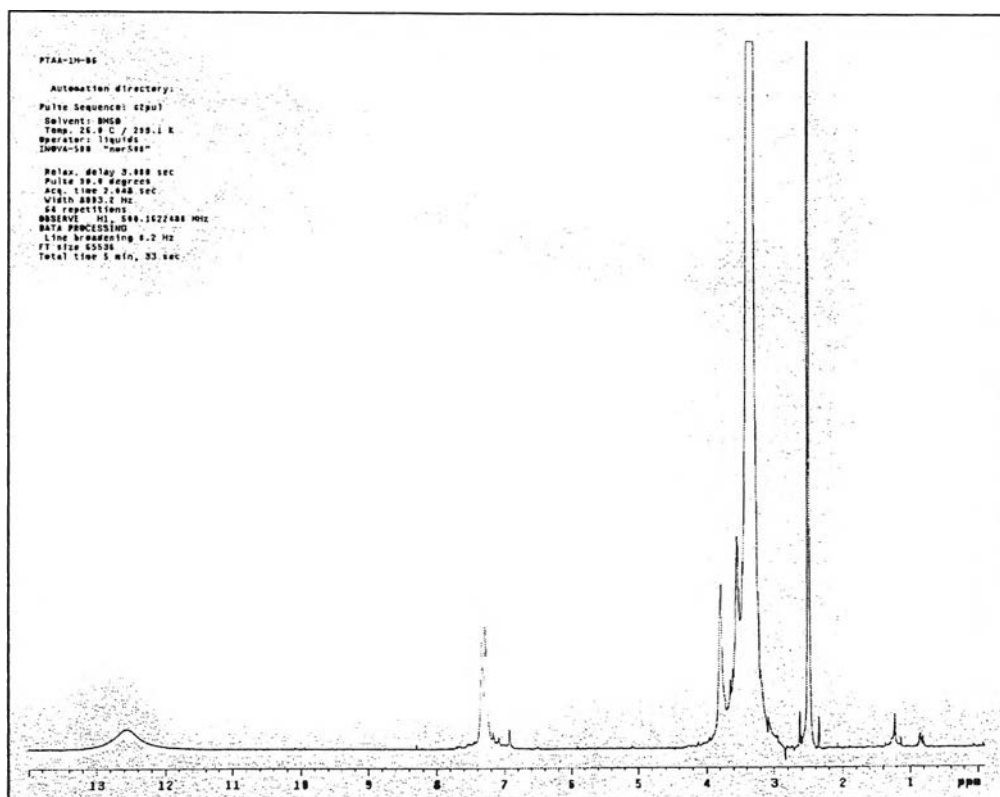
Figure B2 ¹H-NMR characteristic peaks of poly(3-thiophene acetic acid).

¹H-NMR spectra of these polymers were in agreement with their expected structures: P3TMA (Figure 4.6) δ 7.26-7.3 ppm (m, thiophene ring proton, 1H), 3.68 ppm (s, thiophene ring -CH2-, 2H), 3.66 ppm (s, -CH3, 3H). P3TAA Figure 4.7), (DMSO) 12.60 ppm (s, -COOH, 1H), 7.55-7.28 ppm (m,thiophene ring proton, 1H), 3.80-3.37 ppm (m, thiophene ring -CH2-, 2H). The position at 12.6 ppm is the important feature peak of poly(3-thiopheneacetic acid) in order to identify that the structure can be changed from poly(3-thiophene methyl acetate) to poly(3-thiopheneacetic acid) because this peak disappears in case of poly(3-thiophene methyl acetate) (Kim, *et al.*, 1999).

Appendix C Identification of Characteristic Peaks of Undoped Poly (3-thiophene acetic acid) from UV-Visible Spectroscopy

The UV-Visible spectra of undope polythiophene recorded with a UV-Vis absorption spectrometer (Perkin-Elmer, Lambda 10). Measurements were taken in the absorbance mode in the wavelength range of 200-800 nm. Synthesized PTAA was grinded into a fine powder, dissolved in DMSO at the concentration of 6.0×10^{-5} M and pipetted into the sample holder. Scan speed was 240 mm/min, and a slit width of 2.0 nm using a deuterium lamp as the light source.
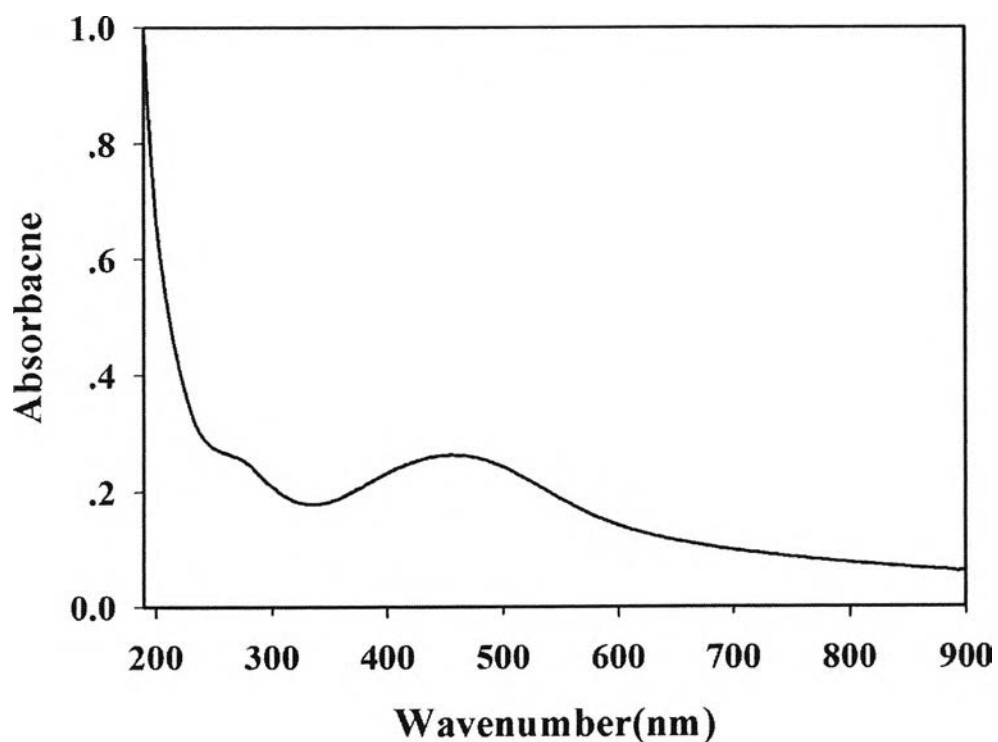
Figure C1 The UV-Visible spectra of; a) undoepd poly(3-thiophene acetic acid).

Appendix D **The Thermogravimetric Thermogram of Undoped poly(3-thiophene acetic acid) and Acrylonitrile-butadiene Rubber**

A thermal gravimetric analyzer (DuPont, model TGA 2950) was used to determine amount decomposition temperature of undoped poly(3-thiophene acetic acid) (P3TAA) and Acrylonitrile butadiene rubber. The temperature scans from 30 to 800°C with a heating rate of 10°C/min. The samples were weighted in the range of 5-10 mg and loaded into a platinum pan, and then heated it under an air flow. Three transitions were observed in undoped poly(3-thiophene acetic acid), 30-120°C, 120-280°C and 280-600°C; they refer to the losses of water and residue solvent, side chain degradation and backbone degradation, respectively (Chotpattananont *et al.*, 2004).
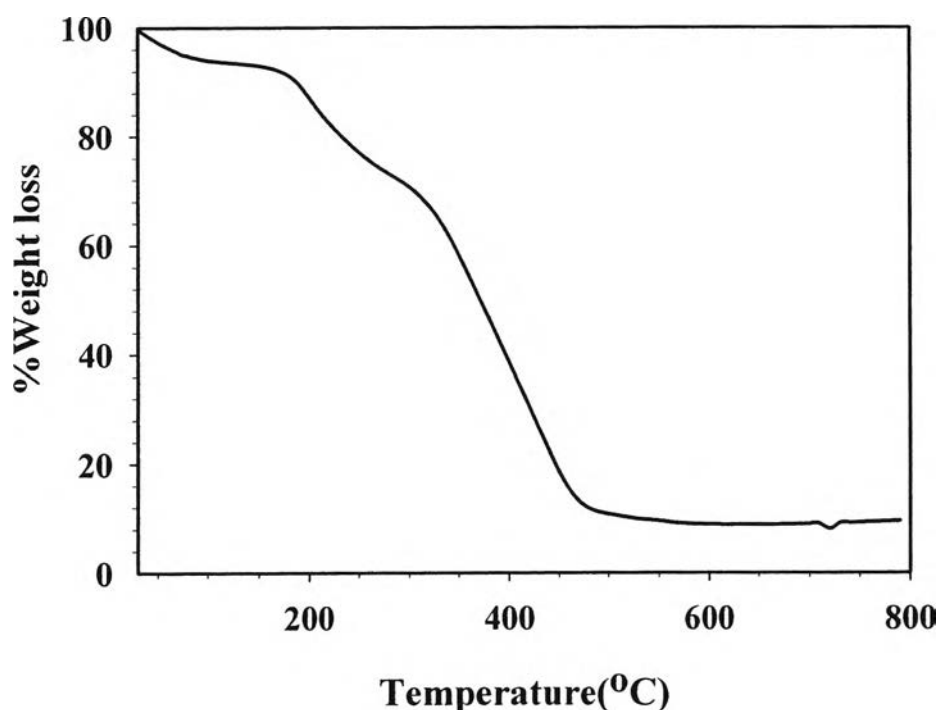

Figure D1 The TGA thermogram of undoped P3TAA under air flow, heating rate10°C/min.

Table D1 Summary of undoped PTAA degradation steps under air flow

Sample	Transition temperature (°C)			% Weight loss			% Residue
	1st	2nd	3rd	1st	2nd	3rd	
Pth_U under air	30-130	130-350	350-650	7.01	25.23	14	53.76

When temperature was scanned from 30 to 800°C with a heating rate of 10°C/min and the samples were weighted in the range of 5-10 mg and loaded into a platinum pan. It was heated under nitrogen gas flow by using Thermogravimetric/differential thermal analyzer (Perkin Elmer, Pyris Diamond). Three transitions were observed in undoped poly(3-thiophene acetic acid), 30-120°C, 120-300 °C and 450-650°C, respectively.
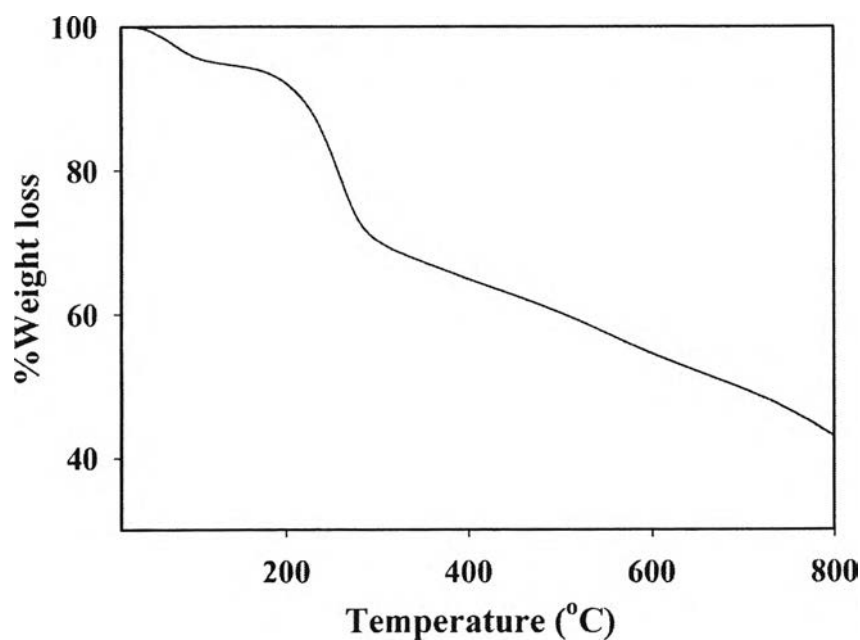
Figure D2 The TGA thermogram of undoped P3TAA under nitrogen flow, heating rate10°C/min.

Table D2 Summary of undoped PTAA degradation steps under nitrogen flow

Sample	Transition temperature (°C)			% Weight loss		
	1st	2nd	3rd	1st	2nd	3rd
Pth_U under Nitrogen gas	30-130	150-330	330-620	7.012	23.27	12.840

For Acrylonitrile butadiene rubber the composites have a better thermal stability. When temperature was scanned from 30 to 800°C with a heating rate of 10°C/min under nitrogen gas and the samples were weighted in the range of 5-10 mg and loaded into a platinum pan. They were heated under nitrogen gas flow. The main transition temperature starts at 415 °C lead to weight loss of 79.84% and completed at 505 °C (George, *et al.*, 2000).
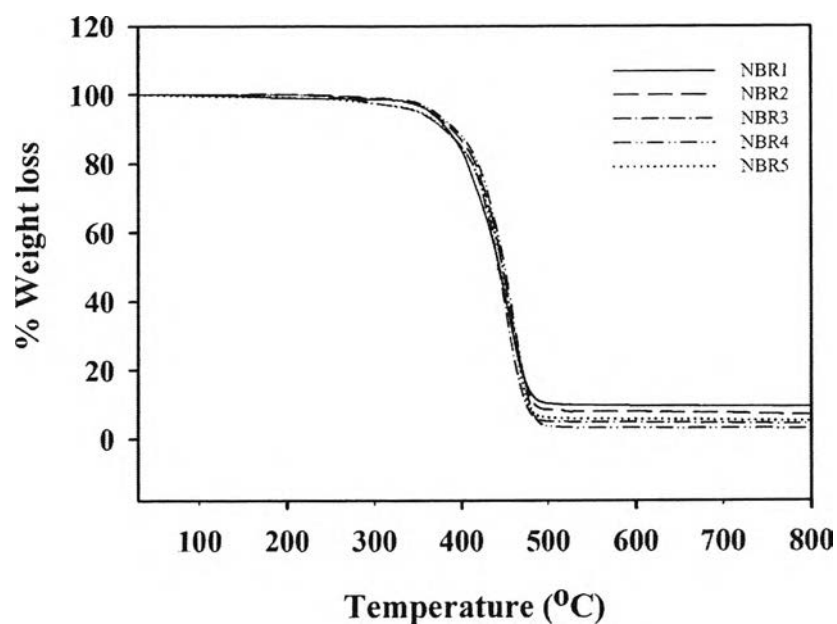
Figure D3 The TGA thermogram of Acrylonitrile butadiene rubber under nitrogen flow, heating rate 10°C/min.
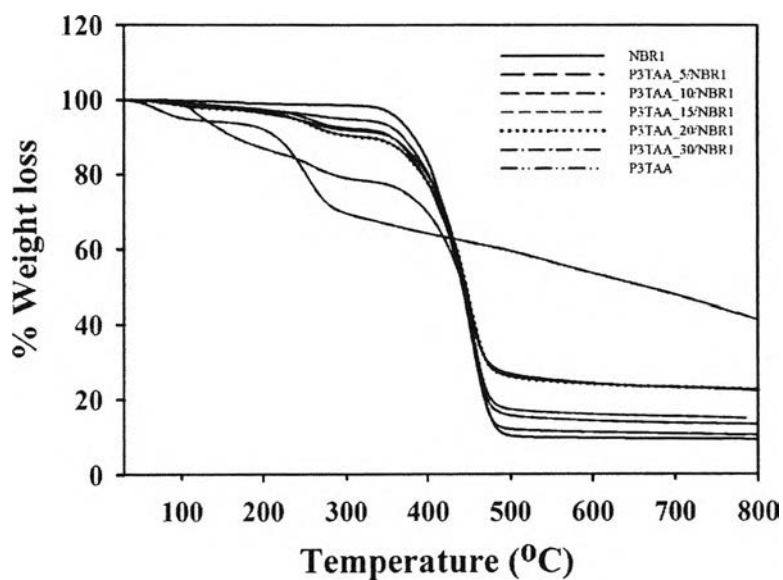
Figure D4 The TGA thermogram of Acrylonitrile butadiene rubber (NBR1) and Poly(3-thiopheneacetic acid)/Acrylonitrile rubber blends under nitrogen flow, heating rate 10°C/min.

Poly(3-thiopheneacetic acid)/Acrylonitrile butadiene rubber, P3TAA/NBR, blends were characterized by using Thermogravimetric/differential thermal analyzer (Perkin Elmer, Pyris Diamond) with a heating rate of 10°C/min from 30 to 800°C under nitrogen gas. At lower concentration of P3TAA, the thermogram of the blend trend to be the same characteristic as pure NBR having a main decomposition temperature around 400 °C. When P3TAA were more added to NBR the thermogram of the blended sample showed decomposition temperature around 230 °C being the decomposition temperature of side chain of P3TAA. When the blends were added more P3TAA the thermogram have the decomposition temperature in between P3TAA and NBR.

Appendix E Conductivity Measurement

The conductivity of matrixes can be measure by using the resistivity testing fixture (Keithley, Model 8009) connected to a source meter (Keithley, Model 6517A) for a constant voltage source and reading resultant current under the atmospheric pressure, 54-60% relative humidity and 24-25°C. The volume resistivity (ρ_v) of matrixes can calculate by following the ASTM standard D257:

$$\rho_v = \frac{K_v}{t} R \qquad \text{(D.1)}$$

where R   is the volume resistance is ohms.

t   is the average thickness of the sample.

K_v is the effective area of the guarded electrode for the particular electrode arrangement employed.

For the Model 8009, which uses circular electrodes, K_v is calculated as follows:

$$K_v = \pi \left(\frac{D\phi}{2} + \beta \frac{g}{2} \right)^2 \qquad \text{(D.2)}$$

D∅ is the effective diameter of the guarded electroded (5.40 cm or 2 ⅛ in).

β   is the effective area coefficient (typically zero).

g   is the distance between the guarded electroded and the ring electrode(⅛ in.).

When β = ∅, the K_v calculation is simplified as follows:

$$K_v = \pi \frac{(D\phi)^2}{4}$$

$$\text{(D.3)}$$

Thus,

$$K_v = \pi \frac{(5.40)^2}{4} = 22.9 cm^2 \qquad \text{(D.4)}$$

or

$$K_v = \pi \frac{(2.125)^2}{4} = 3.55 \, in^2 \qquad (D.5)$$

By using calculated values for K_v, D.1 then becomes:

$$\rho_v = \frac{22.9}{t_c} R \qquad (D.6)$$

or

$$\rho_v = \frac{3.55}{t_i} R \qquad (D.7)$$

where ρ_v is the volume resistivity.

           t_c is the average thickness of the sample in centimeters.

           t_i is the average thickness of the sample in inches.

The applied voltage and the current change in the linear ohmic regime were converted to the electrical conductivity of the polymer by using equation (D.8) as follows:

$$\sigma = \frac{1}{\rho} = \frac{1}{R_s \times t} = \frac{I}{K \times V \times t} \qquad (D.8)$$

Therefore, the electrical conductivity:

$$\sigma = \frac{1}{\rho_v} = \frac{t_c}{22.9R} = \frac{t_c \times I}{22.9 \times V} \qquad (D.9)$$

Where: σ is specific conductivity (S/cm)

           t_c is the average thickness of the sample in centimeters

           I is the measure current (A)

           V is applied voltage (voltage drop) (V)

Table E1 Determination the specific conductivity (S/cm) of Acrylonitrile butadiene rubber

Sample	Conductivity (S/cm)			
	1	2	Average	std
NBR1	3.858E-10	2.768E-10	3.3132E-10	7.709E-11
NBR2	2.819E-10	4.003E-10	3.4108E-10	8.373E-11
NBR3	1.196E-10	3.490E-10	2.3426E-10	1.622E-10
NBR4	1.476E-10	1.152E-10	1.3136E-10	2.291E-11
NBR5	4.299E-10	4.386E-10	4.3424E-10	6.177E-12

From conductivity results, pure NBR rubbers have the electrical conductivity around 10^{-10} S/cm. When undoped P3TAA particles were added to NBR, the conductivity slightly increase around one order magnitude.

Appendix F Scanning Electron Micrograph of Undoped PTAA

Scanning electron microscope (JOEL, model JSM-5200-2AE) was used to determine the morphological structure of the synthesized polymers.

(a)   (b)
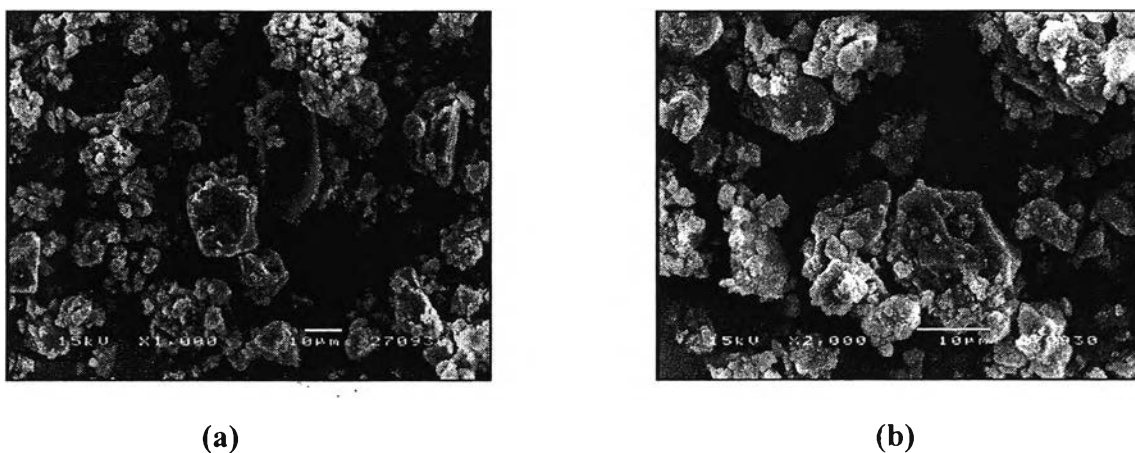
Figure F1 SEM photographs of undope poly(3-thiopheneacetic acid) at magnification: (a)1000; (b)2000.

From the SEM figures, the particle size of P3TAA is around 20 μm. The size of undoped polymers was supported with the results from particle size analyzer from table G1.

From figure E2, the cross cut P3TAA_20/NBR1 sample was checked dispersion of P3TAA in NBR matrix. Figure F2 (b), the sample was extracted the P3TAA particles out of NBR matrix by using pure DMSO to observe dispersion of the particles.

(a)

(b)
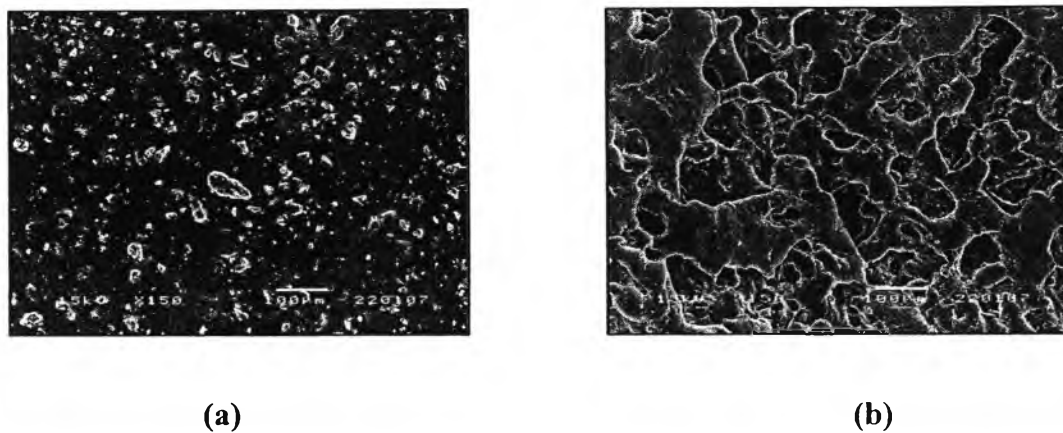
Figure F2 SEM photographs of P3TAA_20/NBR1 blends at magnification 150: (a) cross cut P3TAA_20/NBR1; (b) extracted P3TAA_20/NBR1 with DMSO.

(a)

(b)

(c)

(d)
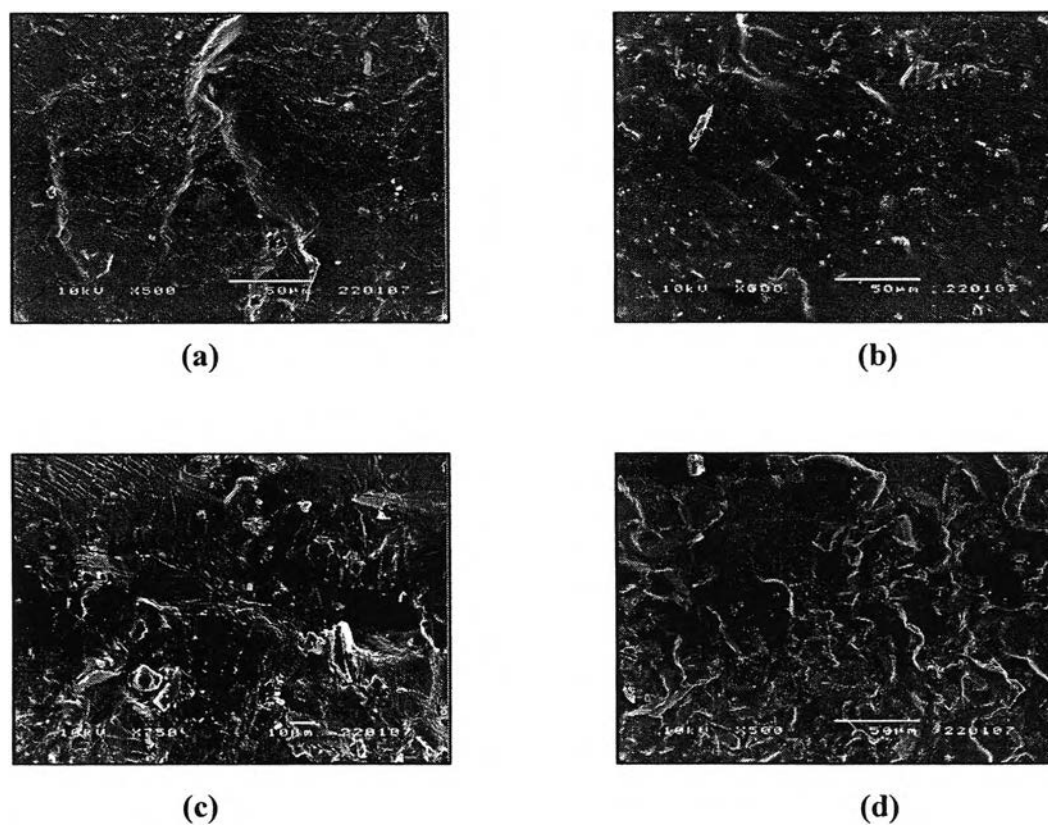
Figure F3 SEM photographs of P3TAA/NBR1 blends at magnification 500: (a) P3TAA_5/NBR1; (b) P3TAA_10/NBR1; (c) P3TAA_20/NBR1; (d) P3TAA_30/NBR1.

Appendix G Determination of Particle Sizes of Undoped and Doped P3TAA

Table G1 Summarized the particles diameter of undoped P3TAA (Pth_U)

Samples	Particle diameter (mm)				
	1	2	3	Avg.	STD
P3TAA	25.03	24.93	25.19	25.05	0.131

Table **G2**   The raw data from particle size analysis of undoped P3TAA

Size		Polythiophene					
		1		2		3	
Low (□m)	High (□m)	In%	Under%	In%	Under%	In%	Under%
0.05	0.12	0.00	0.01	0	0.01	0.00	0.01
0.12	0.15	0.14	0.14	0.13	0.14	0.13	0.13
0.15	0.19	0.27	0.41	0.27	0.40	0.26	0.40
0.19	0.23	0.40	0.81	0.39	0.79	0.39	0.78
0.23	0.28	0.52	1.33	0.52	1.31	0.51	1.29
0.28	0.35	0.64	1.97	0.63	1.94	0.62	1.91
0.35	0.43	0.74	2.71	0.72	2.66	0.71	2.62
0.43	0.53	0.81	3.51	0.79	3.46	0.77	3.39
0.53	0.65	0.84	4.35	0.82	4.28	0.80	4.19
0.65	0.81	0.81	5.17	0.79	5.07	0.77	4.96
0.81	1.00	0.72	5.89	0.70	5.77	0.67	5.63
1.00	1.23	0.59	6.47	0.57	6.34	0.54	6.17
1.23	1.51	0.48	6.96	0.47	6.81	0.44	6.62
1.51	1.86	0.48	7.44	0.46	7.27	0.44	7.05
1.86	2.30	0.58	8.01	0.56	7.83	0.53	7.59
2.30	2.83	0.77	8.79	0.75	8.58	0.72	8.31
2.83	3.49	1.05	9.84	1.03	9.62	1.00	9.31
3.49	4.30	1.41	11.24	1.40	11.01	1.36	10.66
4.30	5.29	1.85	13.09	1.84	12.86	1.80	12.46
5.29	6.52	2.36	15.45	2.36	15.22	2.31	14.78
6.52	8.04	2.94	18.39	2.94	18.16	2.90	17.68
8.04	9.91	3.62	22.01	3.62	21.78	3.58	21.26
9.91	12.21	4.48	26.49	4.47	26.25	4.45	25.70
12.21	15.04	5.68	32.18	5.66	31.92	5.65	31.35
15.04	18.54	7.34	39.52	7.32	39.23	7.32	38.66
18.54	22.84	9.45	48.98	9.46	48.70	9.47	48.14
22.84	28.15	11.40	60.37	11.50	60.20	11.52	59.66
28.15	34.69	12.41	72.77	12.63	72.82	12.69	72.34
34.69	42.75	11.47	84.23	11.78	84.60	11.89	84.23
42.75	52.68	8.80	93.03	9.03	93.63	9.17	93.40
52.68	64.92	5.25	98.27	5.17	98.79	5.29	98.68
64.92	80.00	1.71	100.00	1.19	100.00	1.30	100.00

Appendix H   Electrorheological Properties and Dielectric Properties Measurement of Pure Acrylonitrile-butadiene Rubber and Poly(3-thiopheneacetic acid)/ Acrylonitrile-butadiene Rubber Blend

The electrorheological properties of pure Arylonitrile butadiene rubber were measure by the melt rheometer (Rheometric Scientific, ARES) under oscillatory shear mode and applied electric filed strength varying from 0 to 2 kV/mm. In these experiments, the dynamic moduli (G' and G") were measured as functions of frequency and electric field strength. Strain sweep tests were first carried out to determine the suitable strain to measure G' and G" in the linear viscoelastic regime. As the figure H1 was shown, the linear regime when without electric field was 0.1 % strain.

(a)
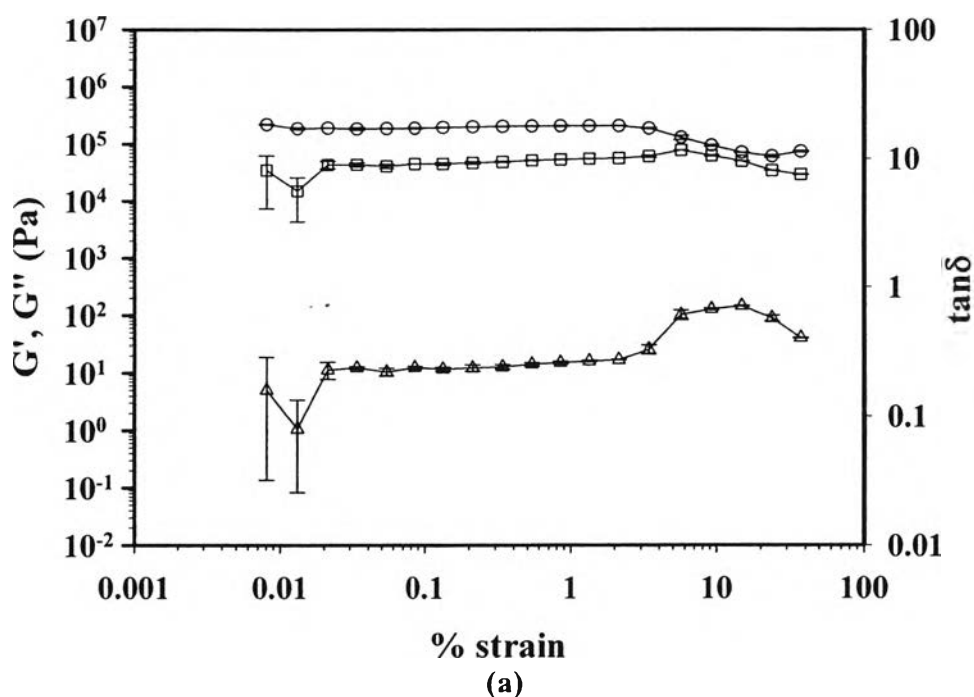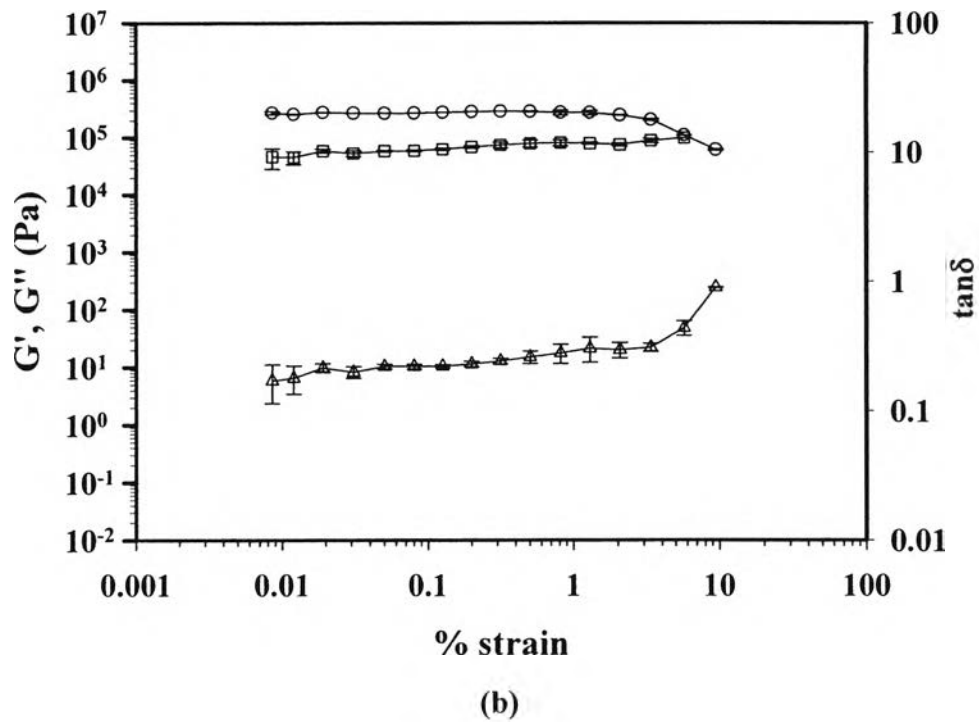
Figure H1 Strain sweep tests of pure arylonitrile-butadiene rubber (NBR1), frequency 1.0 rad/s, temperature 27±0.5 °C, gap = 0.981 mm at: (a) E = 0 kV/mm;(b) E = 2 kV/mm.
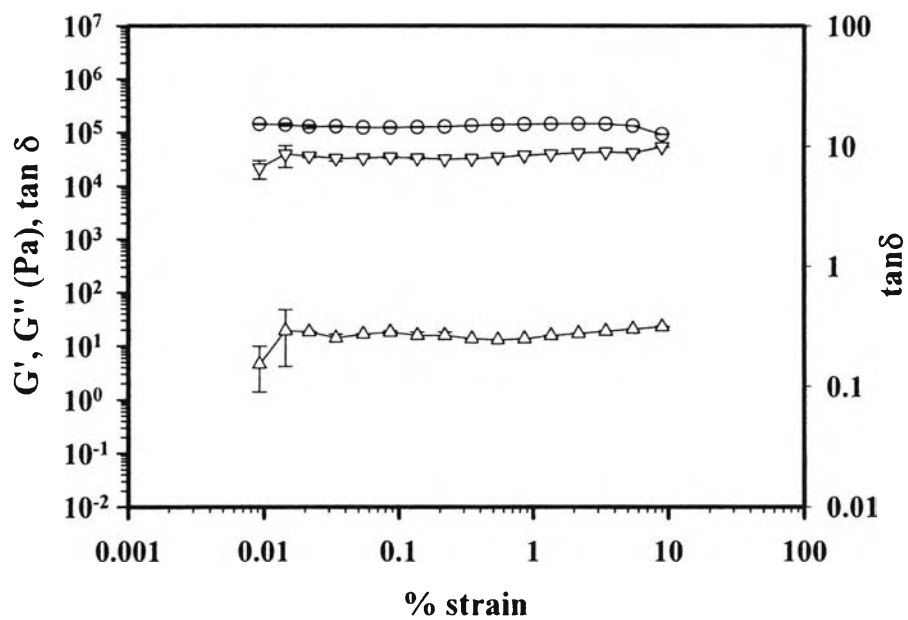
(a)
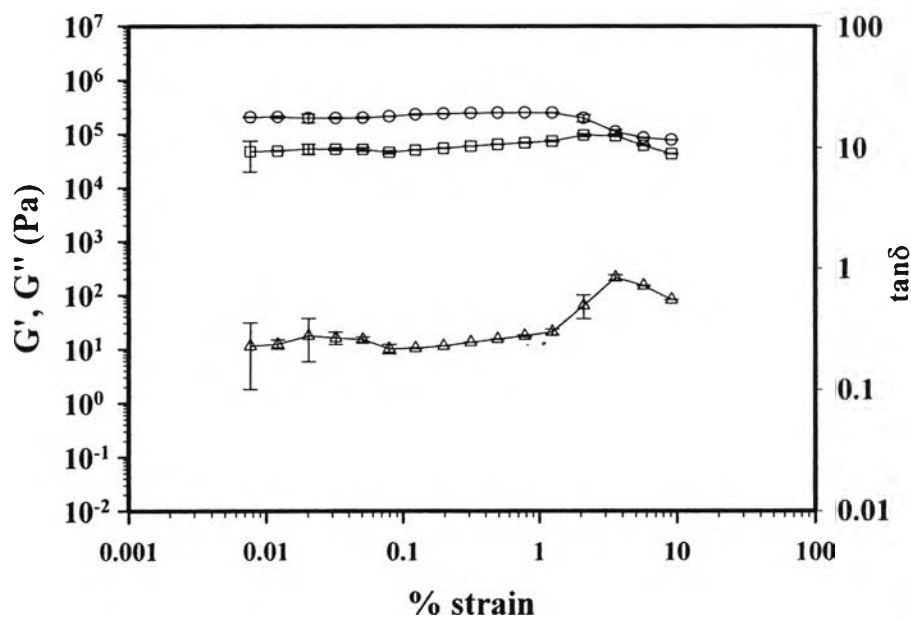
(b)

Figure H2 Strain sweep tests of P3TAA_5/NBR1, frequency 1.0 rad/s, temperature 27±0.5 °C, gap = 0.768 mm at: (a) E = 0 kV/mm; (b) E = 2 kV/mm.
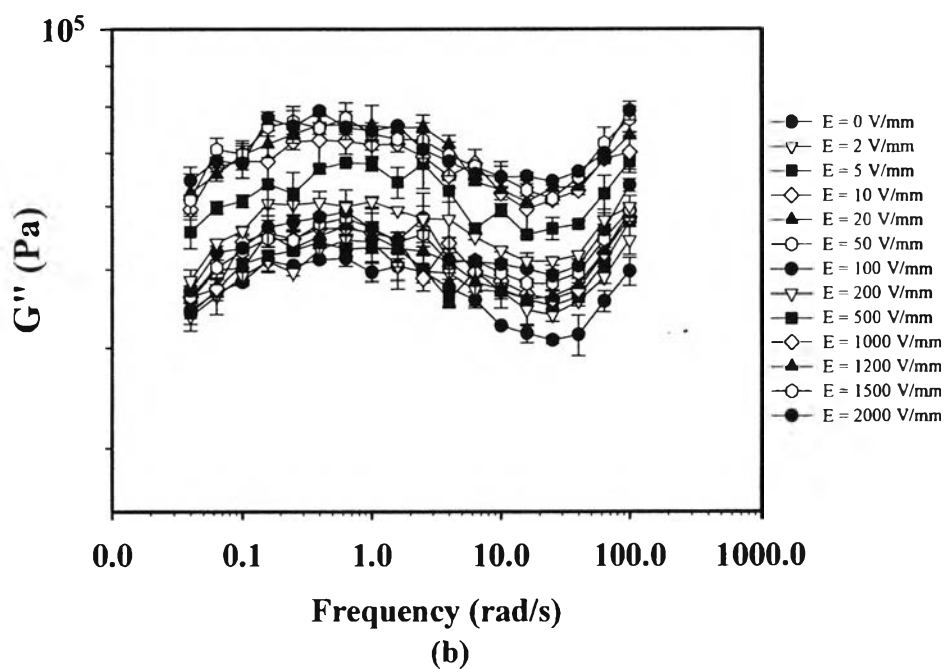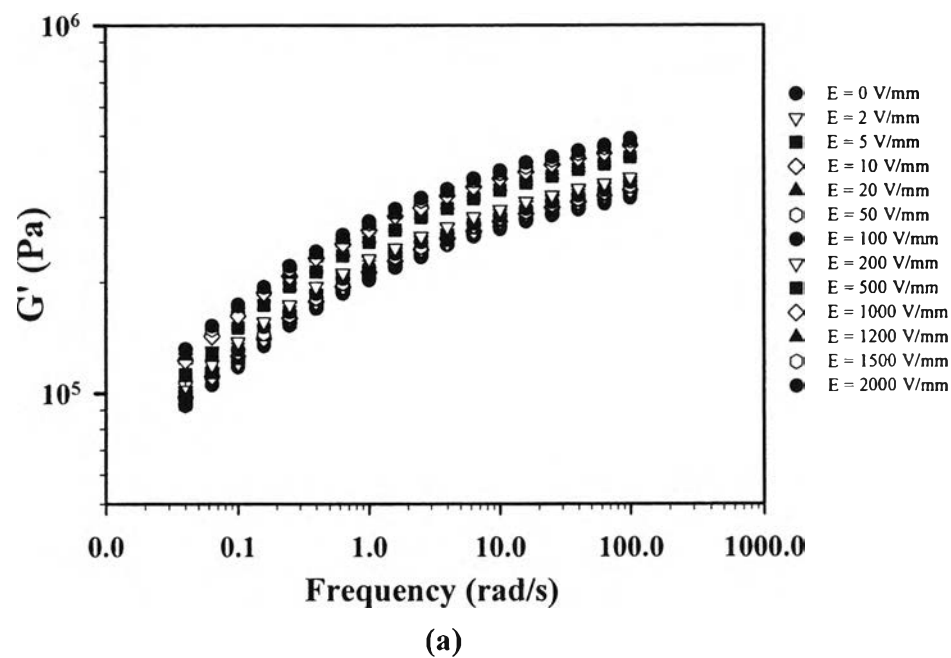
Figure H3 Storage and loss moduli of pure NBR1 at various electric field strengths vs. frequency, strain 0.1%, temperature 27±0.5 °C, gap = 0.981 mm at: (a) storage modulus, $G'(\omega)$; (b) loss modulus, $G''(\omega)$.
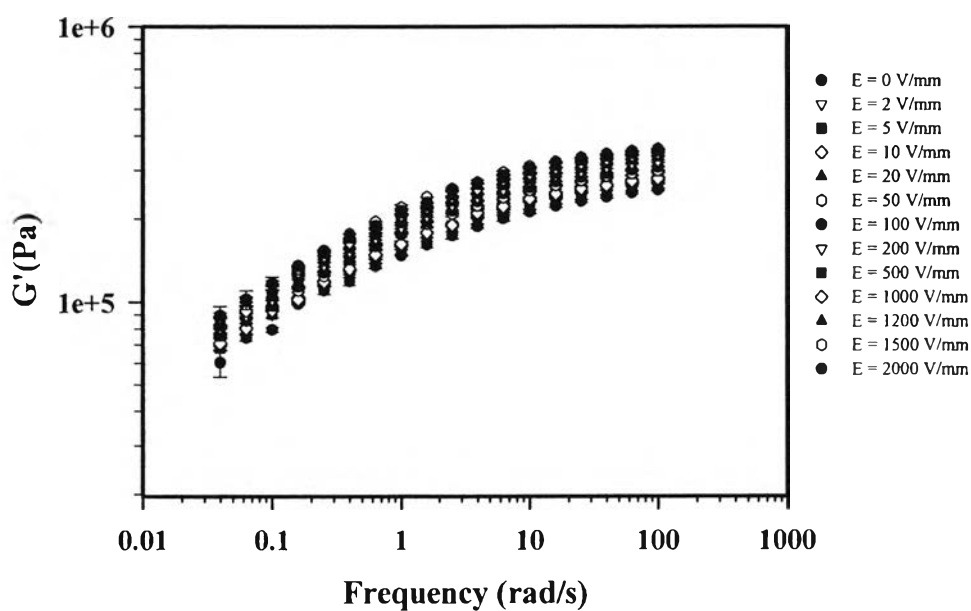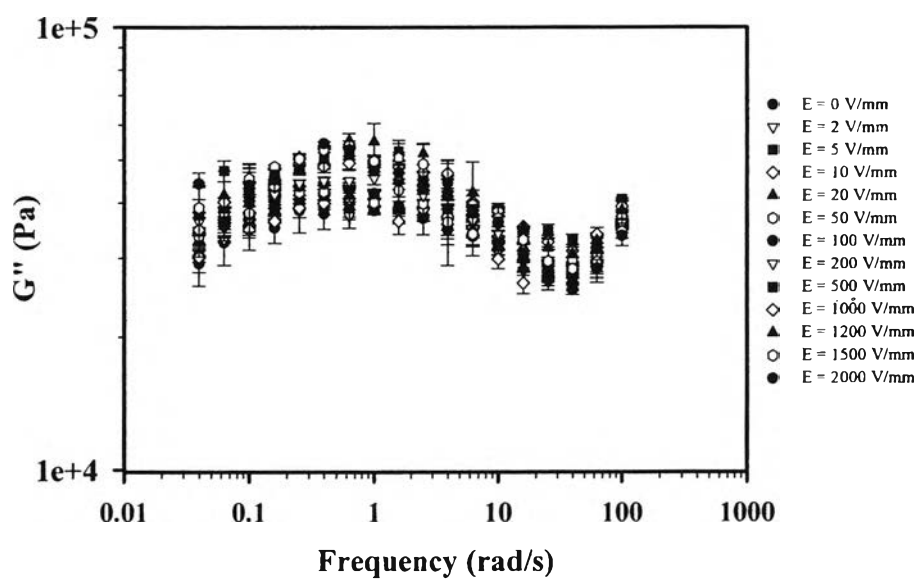
Figure H4 Storage and loss moduli of P3TAA_5/NBR1 at various electric field strengths vs. frequency, strain 0.1%, temperature 27±0.5 °C, gap = 0.768 mm at: (a) storage modulus, $G'(\omega)$; (b) loss modulus, $G''(\omega)$.
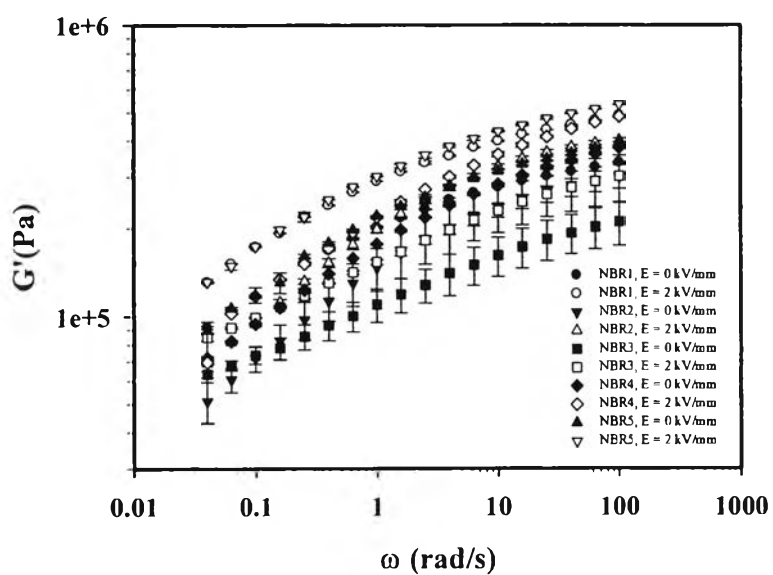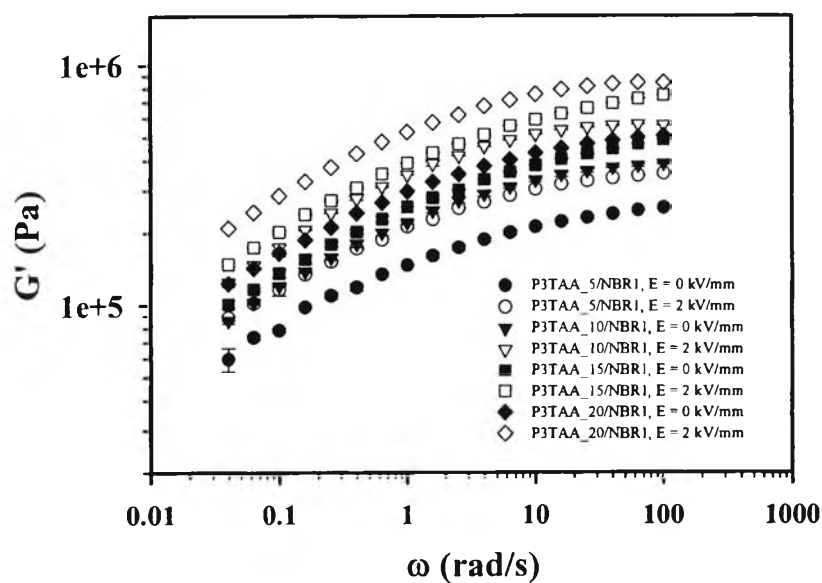
Figure H5 Comparison of the storage modulus (G′) of pure NBR and P3TAA/NBR blends at electric field strength of 0 kV/mm and 2 kV/mm vs. frequency, strain 0.1%, temperature 27±0.5 °C, gap range 0.7- 1.0 mm: (a) pure NBR; (b) P3TAA/NBR.
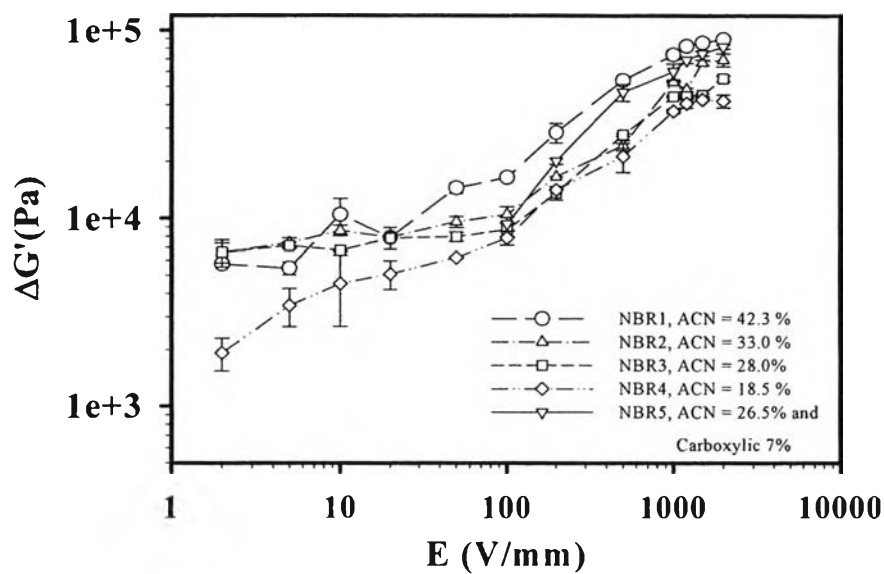
(a)
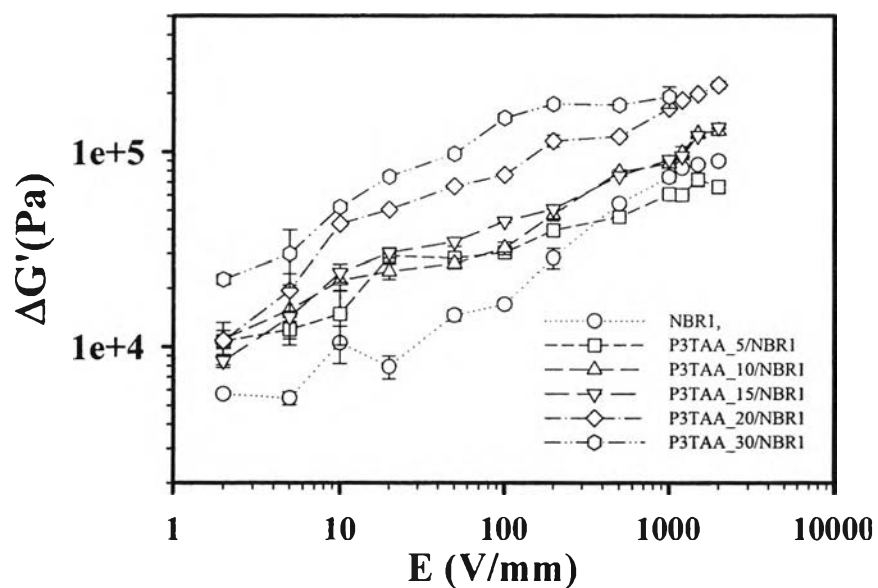
(b)

Figure H6 Comparison of the storage modulus response ($\Delta G'$) of pure NBR and P3TAA/NBR blends at frequency 1.0 rad/s vs. electric filed strength, strain 0.1%, temperature 27±0.5 °C, gap range 0.7- 1.0 mm: (a) pure NBR; (b) P3TAA/NBR.
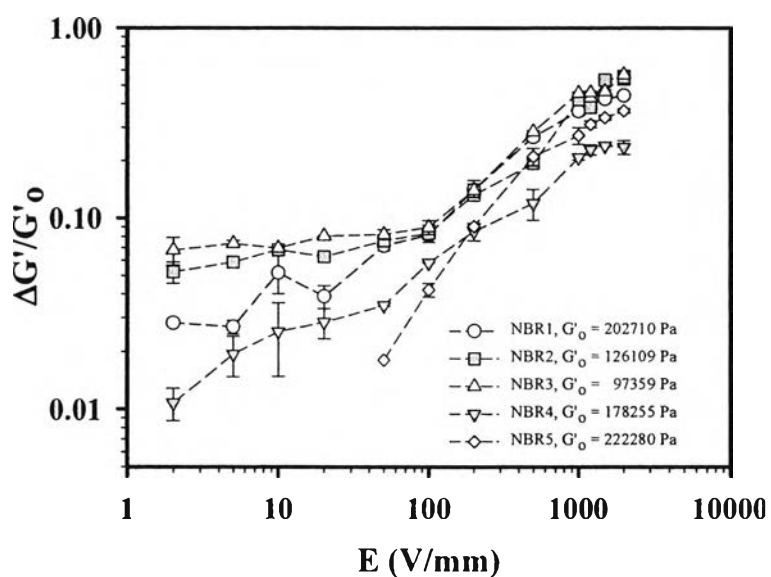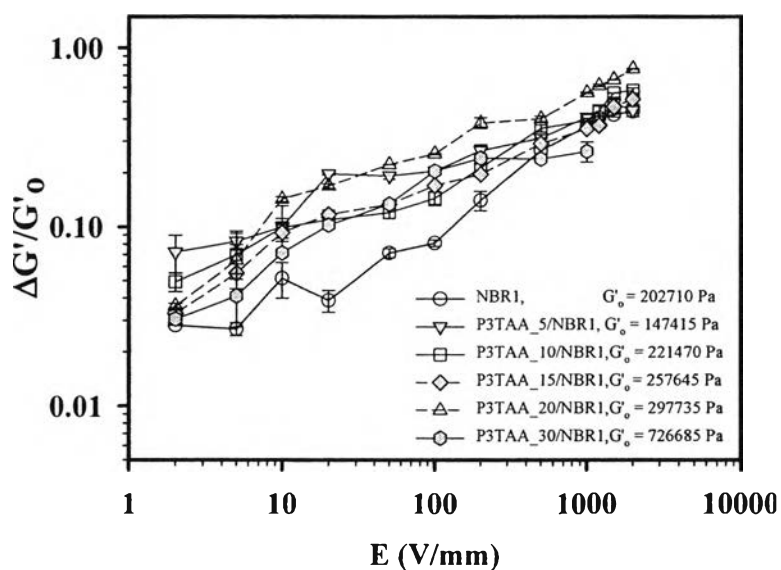
Figure H7 Comparison of the storage modulus sensitivity ($\Delta G'/G'_o$) of pure NBR and P3TAA/NBR at frequency 1.0 rad/s vs. electric filed strength, strain 0.1%, temperature 27±0.5 °C, gap range 0.7- 1.0 mm: (a) pure NBR; (b) P3TAA/NBR.
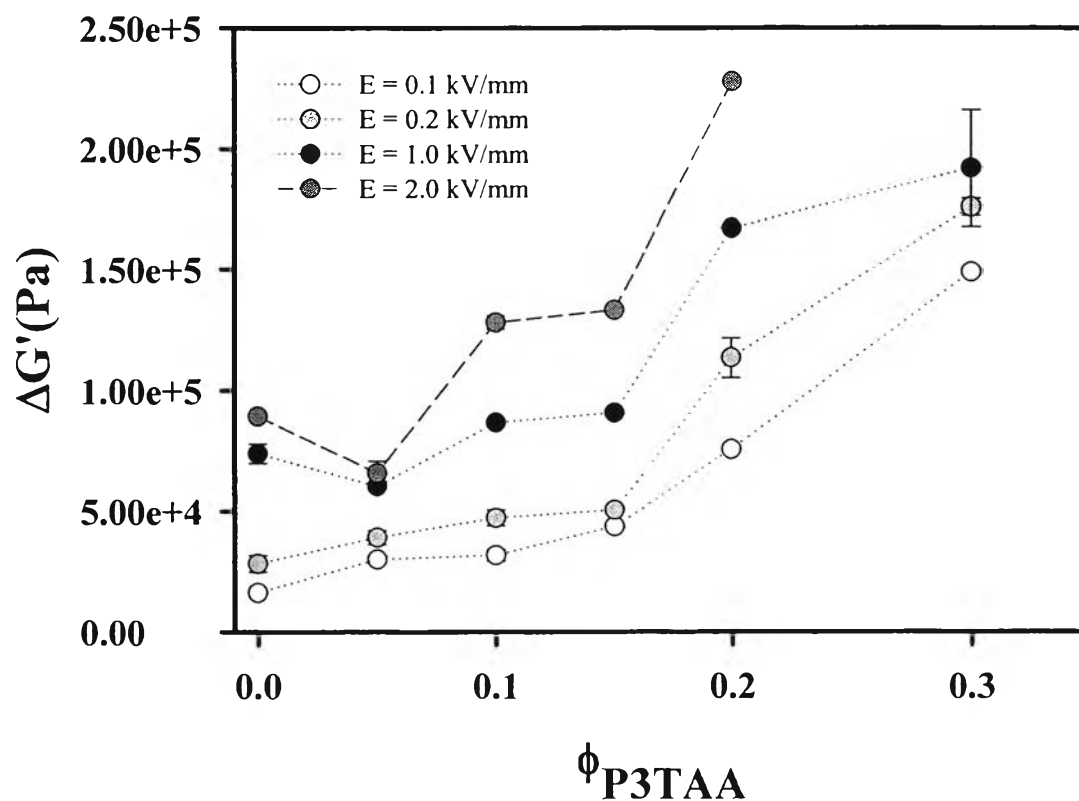
Figure H8 Comparison of the storage modulus response (ΔG') of pure NBR and P3TAA/NBR1 blends at various electric field strengths (0.1, 0.2, and 1 kV/mm) vs. particle concentrations (φ = 0, 5, 10, 15, 20, and 30 %vol.) frequency 1.0 rad/s, strain 0.1%, and temperature 27±0.5 °C.
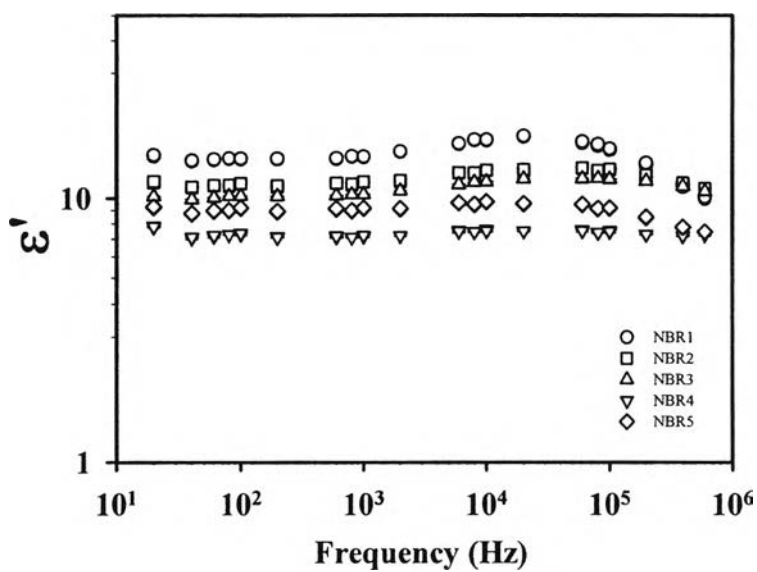
(a)
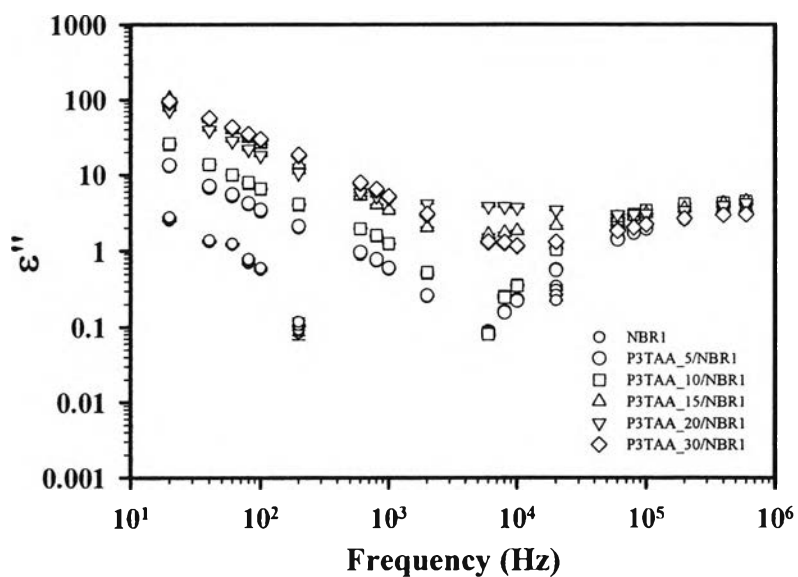
(b)

Figure H9 Comparison of the dielectric constant (ε') and dielectric loss (ε'') of pure NBR vs. frequency at applied volt = 1.0 volt, temperature 27 ± 0.5 °C, gab range 0.7– 1.0 mm: (a) the dielectric constant, (ε'); (b) dielectric loss (ε'').
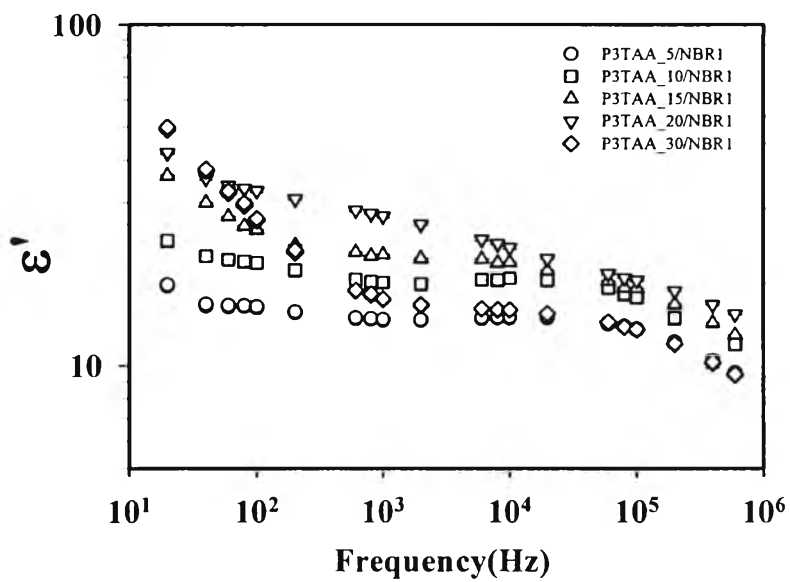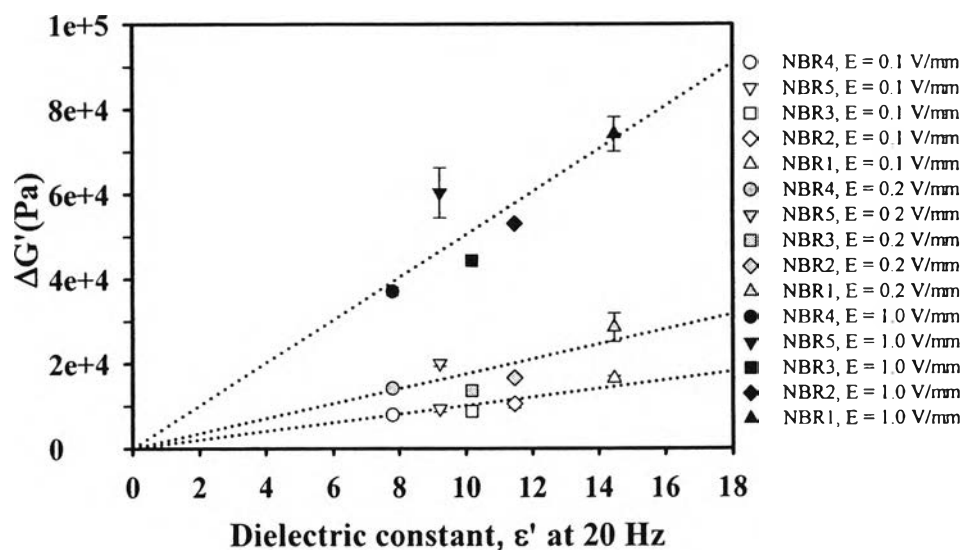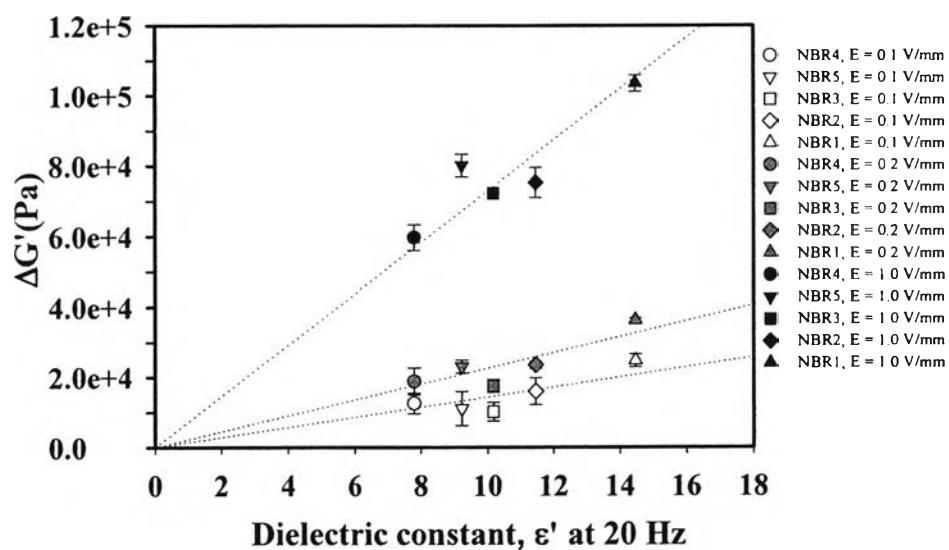
(a)
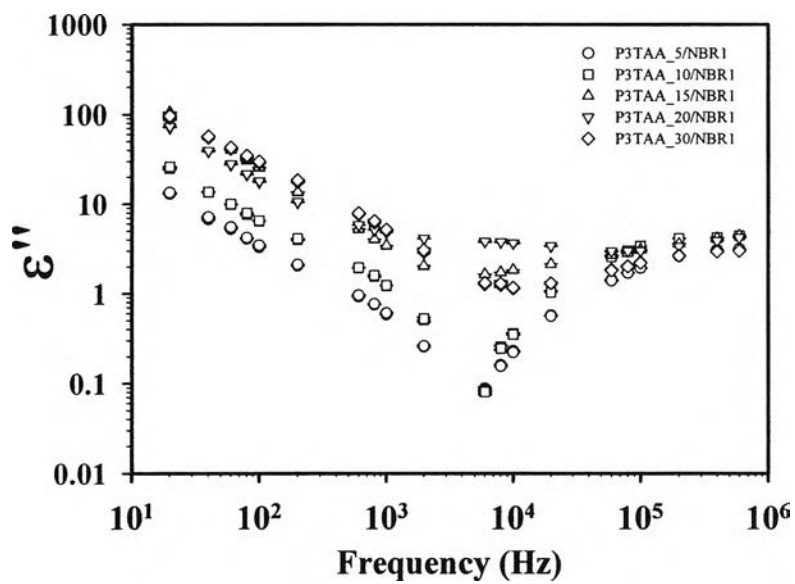
(b)

Figure H10 Comparison of the dielectric constant (ε') and dielectric loss (ε'') of P3TAA/NBR blends vs. frequency at applied volt = 1.0 volt, temperature 27 ± 0.5°C, gab range 0.7 – 1.0 mm: (a) the dielectric constant, (ε'); (b) dielectric loss (ε'').
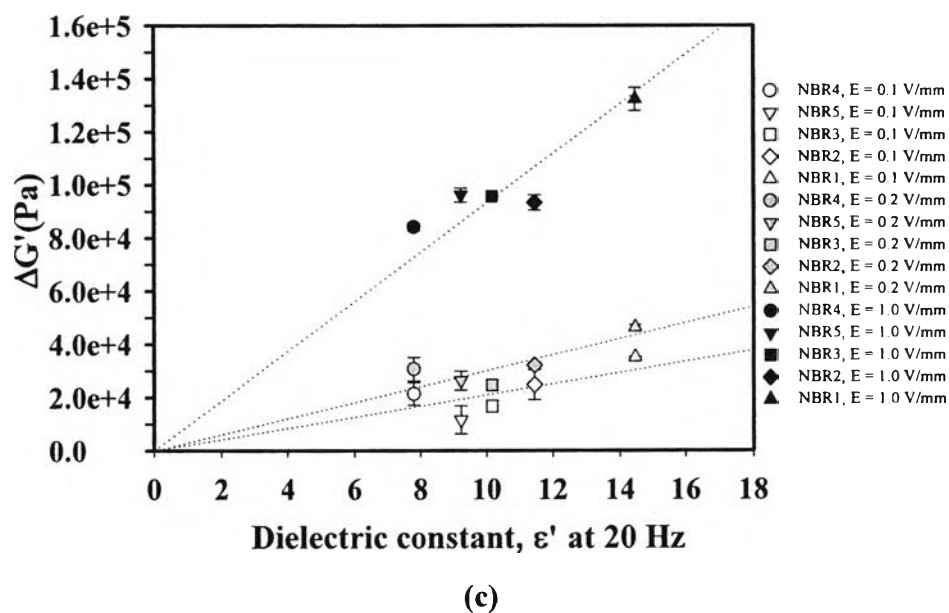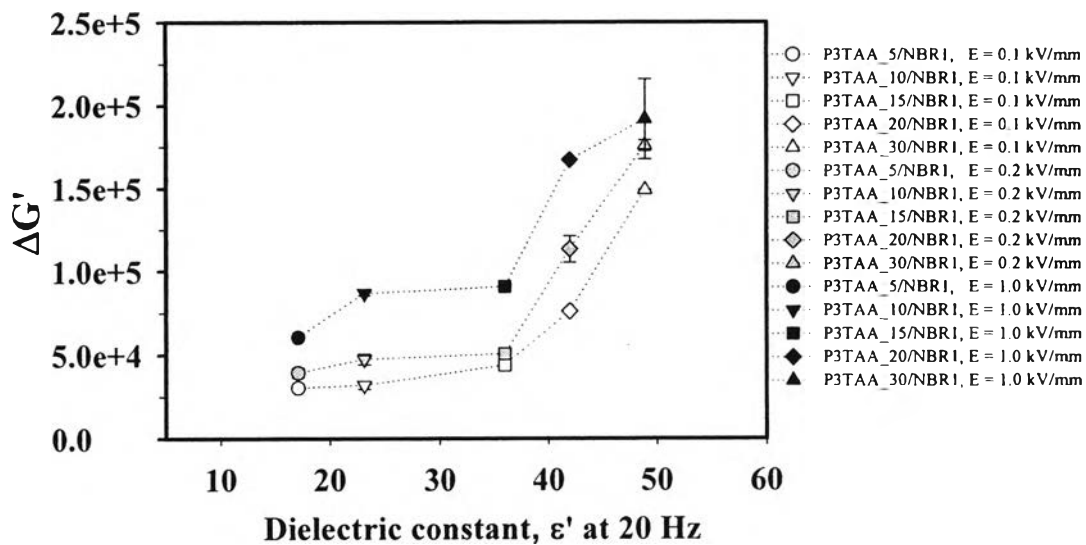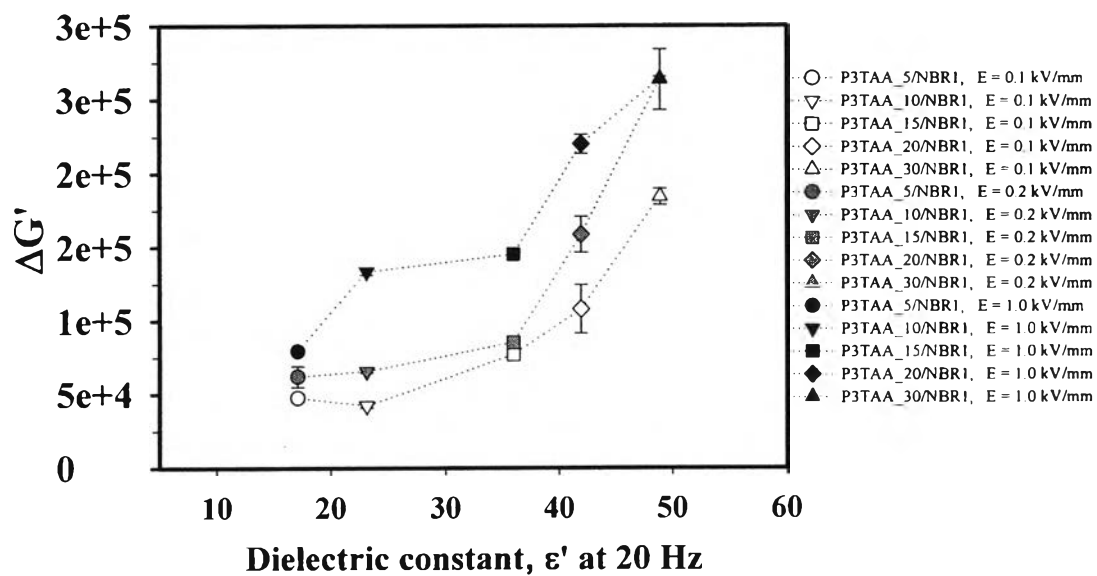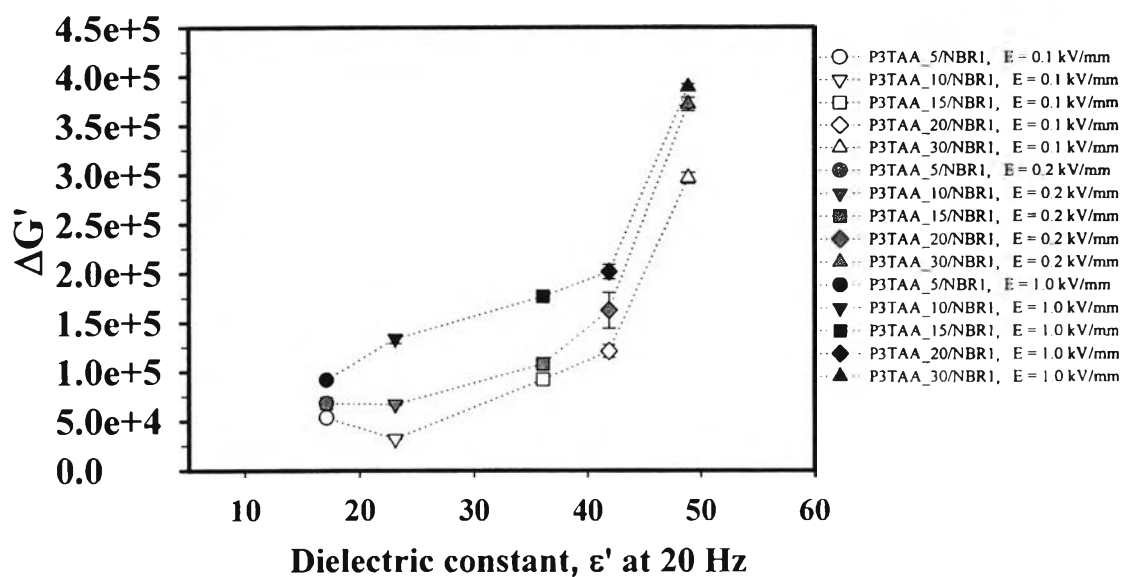
(a)

(b)

(c)

Figure H11 Comparison of the storage modulus response (ΔG') at various frequency (1.0, 10, and 100 rad/s), strain 0.1%, vs. dielectric constant (ε') of pure NBR at applied volt = 1.0 volt, 20 Hz, temperature 27 ± 0.5 °C, gab range $0.7 - 1.0$ mm: (a) 1.0 rad/s; (b) 10.0 rad/s; (c) 100.0 rad/s.

(a)

(b)

Figure H12 Comparison of the storage modulus response (ΔG') at various frequency (1.0, 10, and 100 rad/s), strain 0.1%, vs. dielectric constant (ε') of P3TAA/NBR1 blends at applied volt = 1.0 volt, 20 Hz, temperature 27 ± 0.5 °C, gab range 0.7 – 1.0 mm: (a) 1.0 rad/s; (b) 10.0 rad/s; (c) 100.0 rad/s.

(a)

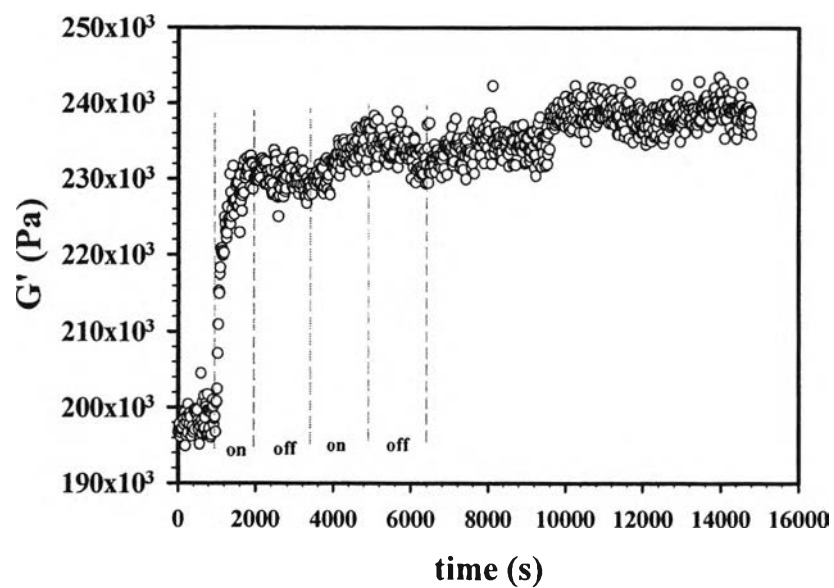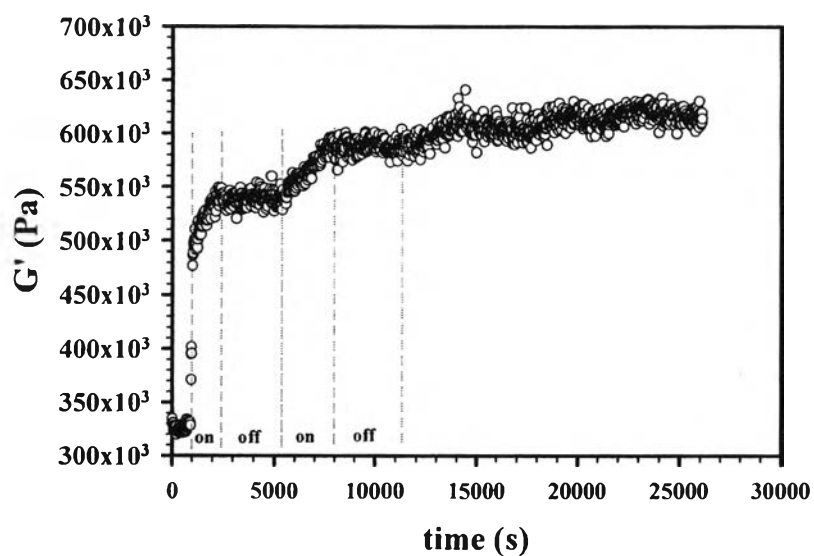**(b)**

Figure H13 Temporal response of the storage modulus (G′) at electric field strengths 1.2 kV/mm vs. time (s), frequency 1.0 rad/s, strain 0.1% and at 27°C of: (a) Pure NBR1; (b) P3TAA_20/NBR1 blends.
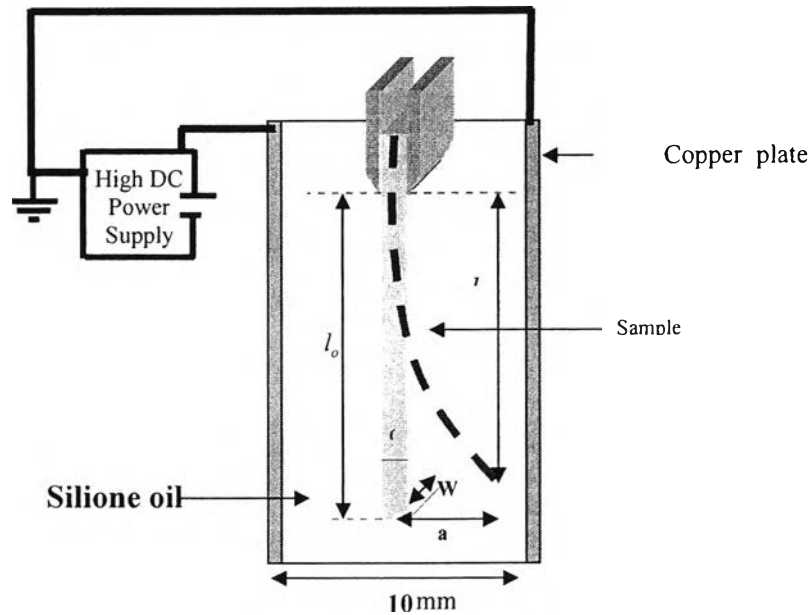
Figure H14 Schematic diagram of the bending response measurement of pure NBR1 and P3TAA_10/NBR1 films suspended vertically in a silicon oil bath and sandwiched between copper plates (30 mm long, 30 mm wide, and 1.0 mm in thickness, the distance between the electrodes is 10 mm) in acrylic box. A DC electric field was applied horizontally at ambient temperature, which causes a deflection distance (a) of the film from its original position to a new position (dash line).

The electric response of the specimens was recorded by a video camera, and the deflection was analyzed by a digital image software (Sciion Image).

Bending angle can be calculated from: (H.1)

$$\tan^{-1}\left(\frac{a}{l}\right)$$

The electric force (F_E) which was calculated from the equation following:

$$F_E = mg\sin\theta + P_E(\theta) \qquad (H.2)$$

where m is the sample's weigth (kg), g is the gravity (9.8 m/s^2), θ is the bending angle, and P_E is the load force (N) from the field which was calculated from [24]:

$$P_E = \frac{3EIa}{l_o^3} \qquad (H.3)$$

where E is Yong's modulus equal to $2G'(1+\upsilon)$, G' is the shear modulus , υ is posson's ratio equal to $1/2$ incompressible, I is the moment of inertia equal to $2/3C^3W$ which C is the sample thickness, W is the sample width, a is the deflection distance (a), and l is the sample length.

Table H1 Bending response test of NBR1

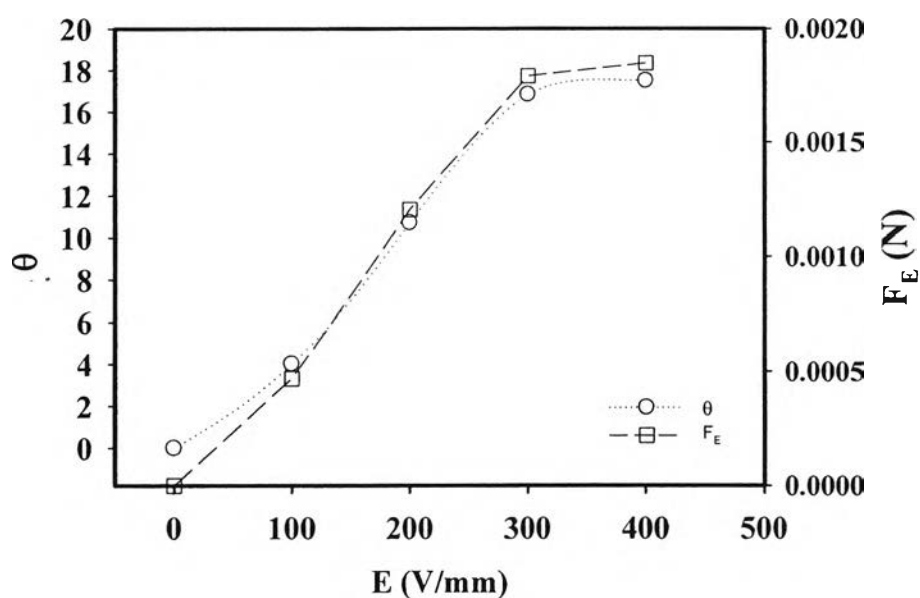| Sample	E (V/mm)	θ (degree)	mgsinθ (N)	P (N)	F$_E$ (N)
NBR1	0	0.00	0.0000E+00	0.0000E+00	0.0000E+00
	100	4.02	1.0404E-04	3.6616E-04	4.7020E-04
	200	10.71	2.7588E-04	9.2872E-04	1.2046E-03
	300	16.82	4.2973E-04	1.3615E-03	1.7912E-03
	400	17.49	4.4621E-04	1.4014E-03	1.8476E-03

Figure H15 Bending angle and electric force of pure NBR1 vs. electric field strength at room temperature. Size of pure NBR sample is 0.6 mm thick, with the weight 0.1515 g, samples 5.55 mm wide.

Table H2 Bending response test of P3TAA_10/NBR1

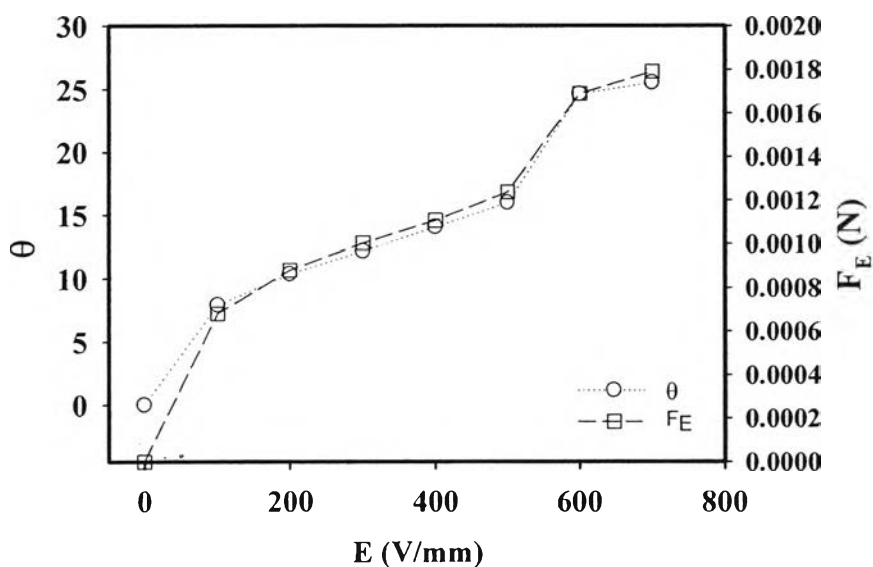| Sample	E (V/mm)	θ (degree)	mgsinθ (N)	P (N)	F_E (N)
P3TAA_10/NBR1	0	0.00	0.0000E+00	0.0000E+00	0.0000E+00
	100	7.92	1.8766E-04	4.9322E-04	6.8088E-04
	200	10.36	2.4504E-04	6.3448E-04	8.7952E-04
	300	12.15	2.8668E-04	7.1589E-04	1.0026E-03
	400	14.06	3.3103E-04	7.7574E-04	1.1068E-03
	500	15.97	3.7489E-04	8.6194E-04	1.2368E-03
	600	24.61	5.6729E-04	1.1229E-03	1.6902E-03
	700	25.53	5.8707E-04	1.2043E-03	1.7914E-03

Figure H16 Bending angle and electric force of P3TAA_10/NBR1 vs. electric field strength at room temperature. Size of P3TAA_10/NBR1 is 0.5 mm thick, weight of 0.1356 g, samples 5.55 mm wide.

CURRICULUM VITAE

Name: Ms. Pacharavalee Thipdech

Date of birth: November 10, 1981

Nationality: Thai

University Education:

       2000 -2004 Bachelor Degree of Industrial Chemistry, Faculty of Science, King Mongkut Institute of Technology Ladkrabang, Bangkok, Thailand.

Working Experience:

       2004   Position: Production Engineer

                        Company name: Mitsui Hygiene Materials (Thailand)